https://doi.org/10.1093/plcell/koad072 THE PLANT CELL 2023: 35: 2027–2043

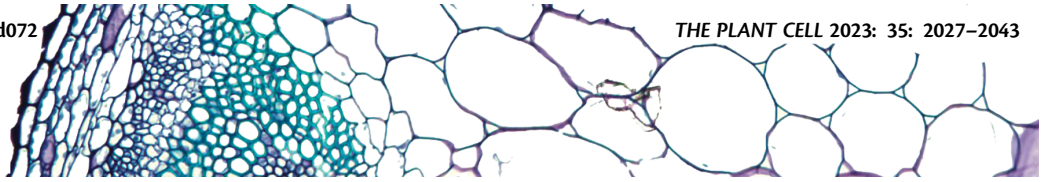

Research Article

Inhibition of SIZ1-mediated SUMOylation of HOOKLESS1 promotes light-induced apical hook opening in Arabidopsis

Jiawei Xiong,† Fabin Yang,† Fan Wei, Feng Yang, Honghui Lin and Dawei Zhang *

Ministry of Education Key Laboratory for Bio-Resource and Eco-Environment, College of Life Science, State Key Laboratory of Hydraulics and Mountain River Engineering, Sichuan University, Chengdu 610064, P.R. China

*Author for correspondence: zhdawei@scu.edu.cn
†These authors contributed equally.
The author responsible for distribution of materials integral to the findings presented in this article in accordance with the policy described in the Instructions for Authors (https://academic.oup.com/plcell/pages/General-Instructions) is: Dawei Zhang (zhdawei@scu.edu.cn).

Abstract

The apical hook protects cotyledons and the shoot apical meristem from mechanical injuries during seedling emergence from the soil. HOOKLESS1 (HLS1) is a central regulator of apical hook development, as a terminal signal onto which several pathways converge. However, how plants regulate the rapid opening of the apical hook in response to light by modulating HLS1 function remains unclear. In this study, we demonstrate that the small ubiquitin-like modifier (SUMO) E3 ligase SAP AND MIZ1 DOMAIN-CONTAINING LIGASE1 (SIZ1) interacts with HLS1 and mediates its SUMOylation in *Arabidopsis thaliana*. Mutating SUMO attachment sites of HLS1 results in impaired function of HLS1, indicating that HLS1 SUMOylation is essential for its function. SUMOylated HLS1 was more likely to assemble into oligomers, which are the active form of HLS1. During the dark-to-light transition, light induces rapid apical hook opening, concomitantly with a drop in *SIZ1* transcript levels, resulting in lower HLS1 SUMOylation. Furthermore, ELONGATED HYPOCOTYL5 (HY5) directly binds to the *SIZ1* promoter and suppresses its transcription. HY5-initiated rapid apical hook opening partially depended on HY5 inhibition of *SIZ1* expression. Taken together, our study identifies a function for SIZ1 in apical hook development, providing a dynamic regulatory mechanism linking the post-translational modification of HLS1 during apical hook formation and light-induced apical hook opening.

Introduction

Light is one of the most important external stimuli affecting plant development. When seeds are buried in the soil and germinate, the young seedlings undergo skotomorphogenesis, which involves hypocotyl elongation, apical hook formation, and the maintenance of folded and undeveloped cotyledons (Smet et al. 2014; Béziat et al. 2017). Upon the perception of light, hypocotyl elongation largely ceases, the apical hook opens, and the cotyledons open and expand, which is collectively called photomorphogenesis or de-etiolation (Kami et al. 2010). The apical hook minimizes damage to the cotyledons and to the shoot apical meristem when moving through soil particles to reach the soil surface (Mazzella et al. 2014; Beziat and Kleine-Vehn 2018). Apical hook development is a dynamic spatiotemporal event that is coordinated by environmental and phytohormone signals (Wang and Guo 2019). For instance, auxin regulates hypocotyl cell elongation in a biphasic manner. The asymmetric state of auxin signaling between the inner and outer sides of the apical hook results in differential cell expansion, thus forming the typical apical hook structure (Béziat et al. 2017; Beziat and Kleine-Vehn 2018; Du et al. 2022). In addition to auxin, multiple studies have revealed HOOKLESS1 (HLS1) as another central regulator of apical hook development (Lehman et al. 1996; Li et al. 2004), whereby HLS1 constitutes a terminal signal that is subjected to a variety of regulatory inputs (Mazzella et al. 2014; Wang and Guo 2019).

The phytohormone ethylene influences auxin biosynthesis and transport in various tissues (Ruzicka et al. 2007; Stepanova

Received October 12, 2022. Accepted February 12, 2023. Advance access publication March 9, 2023

IN A NUTSHELL

Background: When seeds are buried in the soil and germinate, the young seedlings undergo skotomorphogenesis, in which the elongating shoot forms an apical hook. The apical hook protects cotyledons and the shoot apical meristem from mechanical injuries as the shoot emerges from the soil. After reaching the soil surface, seedlings undergo photomorphogenesis, and the apical hook quickly unfolds to allow the shoot to grow upward. HOOKLESS1 (HLS1) is a central regulator of apical hook development, as a terminal signal onto which several pathways converge.

Question: How do plants regulate the rapid opening of the apical hook in response to light by modulating HLS1 function?

Findings: The small ubiquitin-like modifier (SUMO) E3 ligase SAP AND MIZ1 DOMAIN-CONTAINING LIGASE1 (SIZ1) interacts with HLS1 and mediates HLS1 SUMOylation. SUMOylated HLS1 is more likely to assemble into oligomers, which are the active form of HLS1. Upon exposure to light, HY5 suppresses *SIZ1* transcription, thus decreasing HLS1 SUMOylation and initiating rapid apical hook opening. Our study not only describes 1 post-translational modification of HLS1 but also reveals a rapid mechanism regulating apical hook opening via SIZ1-mediated SUMOylation of HLS1.

Next steps: We will further study other post-translational modifications of HLS1 in response to light, as well as the effects of SUMOylation on other biochemical functions of HLS1.

et al. 2007). Ethylene plays an essential role in apical hook development via ETHYLENE INSENSITIVE3 (EIN3)- and EIN3-LIKE1 (EIL1)-mediated modulation of *HLS1* transcription and asymmetric auxin accumulation in the apical hook region (Guzman and Ecker 1990; Raz and Ecker 1999; An et al. 2012; Beziat and Kleine-Vehn 2018; Wang and Guo 2019). Gibberellic acid (GA) and ethylene cooperatively regulate apical hook formation by eliminating the repression of EIN3/EIL1 imposed by DELLA proteins (An et al. 2012). Jasmonic acid (JA) antagonizes ethylene in regulating apical hook formation in an HLS1-dependent manner (Song et al. 2014; Zhang et al. 2014). Salicylic acid (SA) suppresses *HLS1* transcription via NONEXPRESSER OF PR GENES1 (NPR1)-mediated repression of EIN3/EIL1 during apical hook formation (Huang et al. 2020). Moreover, EIN3/EIL1 and PHYTOCHROME-INTERACTING FACTORs regulate apical hook development by co-regulating a particular set of genes, including *HLS1* (Shi et al. 2018; Zhang et al. 2018; Wang and Guo 2019). In addition to *HLS1* transcriptional regulation, HLS1 oligomerization is critical for its function in apical hook formation (Lyu et al. 2019). Although HLS1 is a central regulator of apical hook development, the regulatory mechanism of HLS1 is still poorly understood.

Small ubiquitin-like modifier (SUMO) modification is a dynamic and reversible post-translational modification implicated in many essential cellular pathways (Morrell and Sadanandom 2019). SUMOylation has pleiotropic effects on cell dynamics by regulating the subcellular localization, stability, protein–protein interaction, and transcriptional activity of its target proteins (Bernula et al. 2020; Srivastava et al. 2020, 2022; Zhang et al. 2020; Zheng et al. 2020). Similar to ubiquitination, SUMOylation is catalyzed by a series of dedicated enzymes (Morrell and Sadanandom 2019). First, SUMO is activated by a heterodimer of the E1 ligases SUMO-ACTIVATING ENZYME1 (SAE1) and SAE2. Second, activated SUMO is transferred from SAE2 to a cysteine residue in SUMO-CONJUGATING ENZYME1 (SCE1), an E2 conjugation enzyme. Finally, SUMO E3 ligases help transfer SUMO from SCE1 to the target substrate (Mukhopadhyay and Dasso 2007; Augustine and Vierstra 2018; Morrell and Sadanandom 2019). SAP AND MIZ1 DOMAIN-CONTAINING LIGASE1 (SIZ1) is one such SUMO E3 ligase that has been reported to affect multiple developmental decisions, including flowering (Jin et al. 2008; Son et al. 2014), seed germination (Kim et al. 2015), abiotic stress responses (Miura et al. 2007; Rytz et al. 2018; Kong et al. 2020), plant immunity (Gou et al. 2017; Niu et al. 2019), and photomorphogenesis (Lin et al. 2016).

Here, we show that SIZ1 positively regulates apical hook formation by SUMOylating HLS1 in Arabidopsis (*Arabidopsis thaliana*). SUMOylated HLS1 is more likely to assemble into active oligomers. Upon exposure to light, HY5 suppresses *SIZ1* transcription, thus decreasing HLS1 SUMOylation and initiating rapid apical hook opening. Our study not only describes 1 post-translational modification of HLS1 but also reveals a rapid regulatory mechanism of apical hook opening via SIZ1-mediated HLS1 SUMOylation.

Results

SIZ1 positively regulates apical hook formation

SIZ1 negatively regulates photomorphogenesis (Lin et al. 2016). To test whether SIZ1 regulates apical hook development, we quantified apical hook curvature in *siz1-2* (*SIZ1* loss-of-function mutant) etiolated (dark-grown) seedlings. The extent of apical hook curvature was significantly lower in *siz1-2* than in the wild-type Columbia-0 (Col-0), while the *SIZ1pro:SIZ1-GFP siz1-2* (*SSG* thereafter) line showed no difference with Col-0, indicating that the SIZ1–green fluorescent protein (GFP) fusion is functional (Fig. 1, A and B). To distinguish between a defect in hook formation or premature hook opening phenotype in *siz1-2*, we observed dynamic apical hook formation from the time of seed germination onward (Supplemental Fig. 1, A and B). We determined that *siz1-2* cannot form an apical hook (Supplemental Fig. 1, A and B).

The *siz1-2* mutant hyperaccumulates SA (Lee et al. 2007b), which was shown to inhibit apical hook formation (Huang et al. 2020). To test whether the defect of apical hook development seen in *siz1-2* was due to its elevated SA levels, we tested the apical hook curvature of *NahG* (expressing a bacterial salicylate hydroxylase that degrades SA) and *NahG siz1-2* seedlings. We determined that the apical hook angle of *NahG* seedlings is similar to that of Col-0, whereas expressing *NahG* in *siz1-2* only partially rescued the formation of an apical hook (Supplemental Fig. 2, A and B), indicating that the elevated SA level of *siz1-2* does not contribute much to its apical hook phenotype.

When buried seedlings are exposed to light, they switch to photomorphogenesis or de-etiolation, which is characterized by unfolding of the apical hook and the opening and expansion of cotyledons (Kami et al. 2010). To assess the mechanism of SIZ1-mediated apical hook development, we measured the dynamic changes in apical hook angle over time following transfer into light. We observed that *siz1-2* seedlings show a faster rate of apical hook opening than Col-0 when exposed to light (Fig. 1, C and D). These results indicate that SIZ1 positively regulates apical hook formation and plays a negative role in light-induced apical hook unfolding.

SIZ1 interacts with HLS1 in vitro and in vivo

As a SUMO E3 ligase, SIZ1 typically modulates the function of target proteins by adding the SUMO modification. To identify the target proteins of SIZ1 during apical hook formation, we performed a yeast 2-hybrid (Y2H) screen using SIZ1 as bait and a cDNA library generated from 3-d-old dark-grown Arabidopsis seedlings as prey, which revealed that SIZ1 interacts with a fragment of HLS1. We then conducted a targeted Y2H assay and determined that full-length HLS1 also interacts with SIZ1 (Fig. 2A). We validated the interaction between SIZ1 and HLS1 by in vitro maltose-binding protein (MBP) pull-down assays, as recombinant MBP-HLS1 pulled down His-SIZ1 when co-incubated (Fig. 2B).

To further validate the interaction of SIZ1 with HLS1, we performed bimolecular fluorescence complementation (BiFC) assays in *Nicotiana benthamiana* leaves. To this end, we co-infiltrated constructs encoding HLS1 fused to the N-terminus of yellow fluorescent protein (nYFP) (*HLS1-nYFP*) with a construct encoding SIZ1 fused to the C-terminus of YFP (cYFP) (*SIZ1-cYFP*). We detected YFP fluorescence in the nucleus, which provided support for the interaction of SIZ1 with HLS1 in planta (Fig. 2C). Co-immunoprecipitation (Co-IP) assays using transgenic seedlings harboring the pair of transgenes *HLS1pro:HA-FLAG-HLS1 SIZ1pro:SIZ1-GFP* and *HLS1pro:HA-FLAG-HLS1 SIZ1pro:GFP* showed that SIZ1 co-precipitates with HLS1 (Fig. 2D). These results demonstrate that SIZ1 interacts with HLS1 in vitro and in vivo.

SIZ1 mediates the SUMOylation of HLS1 in vivo

To investigate whether HLS1 is SUMOylated, we performed an in vitro SUMOylation assay as described previously (Lin et al. 2016; Zhang et al. 2019; Zheng et al. 2020). Accordingly, we incubated recombinant HLS1 with E1 and E2 enzymes and either His-SUMO1^{GG} (the mature form of SUMO1, with the C-terminal double-Gly motif exposed) or His-SUMO1^{AA} (a conjugation-defective SUMO1 mutant, with the double-Gly motif mutated to double-Ala) for the assay. We established that HLS1 can be SUMOylated in vitro even in the absence of SIZ1 (Fig. 3A). We therefore used in vivo SUMOylation assays to validate the SUMOylation of HLS1 observed in vitro. We transiently transfected *HA-HLS1* and *MYC-SUMO1* constructs into Arabidopsis protoplasts prepared from Col-0 or *siz1-2*, followed by immunoblot analysis with anti-HA and anti-MYC antibodies. We detected SUMOylated HLS1 in transfected protoplasts from Col-0 but not from *siz1-2* (Fig. 3B).

To further determine whether SIZ1 mediates the SUMOylation of HLS1 in planta, we generated *35S:HA-FLAG-HLS1* (*HLS1OE*) and *HLS1OE siz1-2* transgenic lines overexpressing *HA-HLS1*. To detect HLS1 SUMOylation in different genotypes, we extracted total proteins from 3-d-old dark-grown seedlings, followed by incubation with HA agarose beads for immunoprecipitation and immunoblot analysis with anti-SUMO1 antibodies. We detected SUMO1-conjugated HLS1 in protein extracts isolated from *HLS1OE* but not from *HLS1OE siz1-2* seedlings (Fig. 3C). These results indicate that SIZ1 mediates the SUMOylation of HLS1 in vivo.

We conducted a bioinformatics analysis using GPS-SUMO (http://sumosp.biocuckoo.org/online.php) and SUMOplot (https://www.abcepta.com/sumoplot) to identify predicted SUMOylation sites in HLS1. These searches identified 6 potential SUMOylation sites in HLS1 (lysine [K] 62, K81, K155, K186, K294, and K336) (Supplemental Fig. 3). To assess the predicted SUMOylation site(s) in HLS1, we generated HLS1 point mutants harboring single substitutions of each K residue to arginine (R) (Supplemental Fig. 3) before performing in vitro and in vivo SUMOylation assays. We observed a reduction in HLS1 SUMOylation levels in all single-mutation mutants (Fig. 3, D and E), suggesting that all 6 K residues are bona fide SUMOylation sites. Interestingly, we failed to detect SUMOylated HA-HLS1 when using an anti-HA antibody in vivo (Fig. 3E). However, this result was expected, as SUMOylation is a reversible modification that can be rapidly removed by SUMO-specific proteases likely present in the protein extracts. SUMOylated HLS1 may thus only represent a small fraction of the total protein (Creton and Jentsch 2010; Saleh et al. 2015).

To explore whether the 6 K residues are critical SUMOylation sites in HLS1, we generated several constructs encoding various HLS1 mutant variants: 2KR (K62 and K81 residues changed to R), 3KR (K62R, K81R, and K155R), 4KR (K62R, K81R, K155R, and K186R), 5KR (K62R, K81R, K155R, K186R, and K294R), and 6KR (K62R, K81R, K155R, K186R, K294R, and K336R) (Supplemental Fig. 3). Subsequent in vitro SUMOylation and in vivo SUMOylation assays showed that HLS1 SUMOylation gradually decreases from 2KR, 3KR, and 4KR to 5KR mutants, as the number of SUMOylation sites diminishes; importantly, HLS1 SUMOylation was abolished in

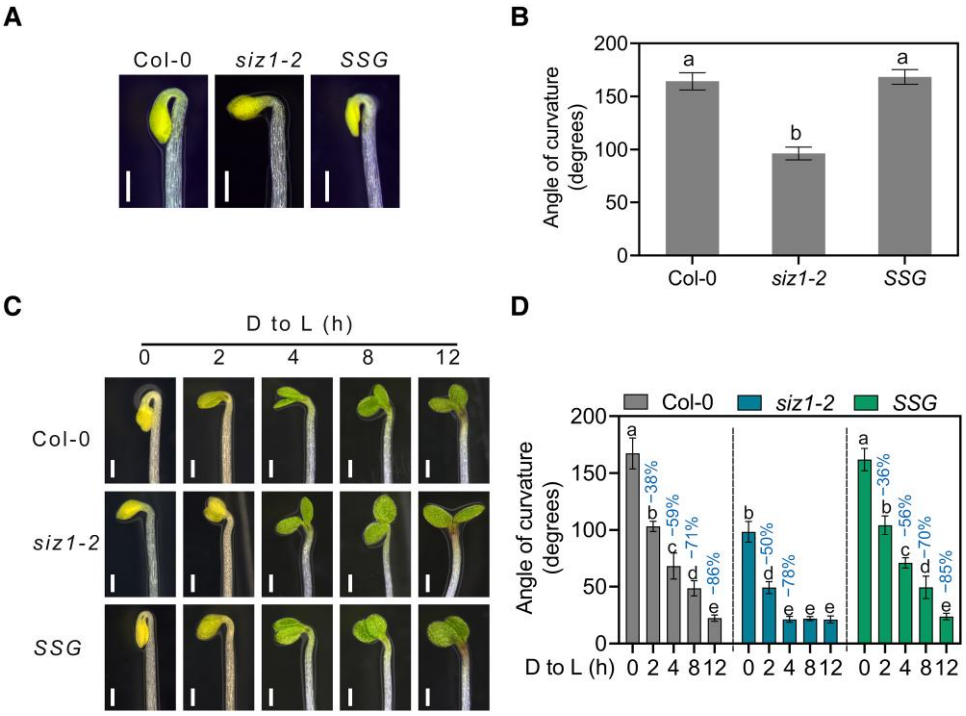

Figure 1. SIZ1 promotes apical hook development. **A)** Apical hook phenotype of 3-d-old dark-grown Col-0, *siz1-2*, and *SIZ1pro:SIZ1-GFP siz1-2* (*SSG*) seedlings. Scale bars, 1 mm. **B)** Quantification of apical hook curvature from seedlings shown in **A)**. Data represent means ± SE from 3 replicates, with each replicate consisting of at least 12 seedlings. Different lowercase letters indicate significant differences ($P < 0.05$) based on 1-way ANOVA followed by Fisher's LSD test. **C)** Apical hook phenotypes of Col-0, *siz1-2*, and *SSG* seedlings. The seedlings were grown on half-strength MS medium in darkness for 3 d and then transferred to light (D to L) for the indicated times. Scale bars, 1 mm. **D)** Quantification of apical hook curvature from seedlings shown in **C)**. Data represent means ± SE from 3 replicates, with each replicate consisting of at least 12 seedlings. Percentages represent the decrease in apical hook angle (light-induced angle/angle before light exposure). Different lowercase letters indicate significant differences ($P < 0.05$) based on 2-way ANOVA followed by Fisher's LSD test.

the 6KR mutant (Fig. 3, F and G). We also generated *35S:HA-FLAG-HLS1*^{K186R} (*HLS1*^{K186R}*OE*) and *35S:HA-FLAG-HLS1*^{6KR} (*HLS1*^{6KR}*OE*) transgenic lines to investigate the effects of the 6KR mutant on HLS1 SUMOylation in planta. We determined that the levels of SUMOylated HLS1 are lower in *HLS1*^{K186R}*OE* relative to the wild type and almost undetectable in *HLS1*^{6KR}*OE* (Fig. 3C). These results indicate that the K62, K81, K155, K186, K294, and K336 residues are the principal targets for HLS1 SUMOylation.

The SUMOylation of HLS1 is essential for its function in apical hook formation

To verify the roles of HLS1 SUMOylation in apical hook development, we generated transgenic lines carrying constructs encoding various mutated forms of HLS1 fused with an HA tag in the *hls1-1* background (*HLS1pro:HA-HLS1* hls1-1*, where * represents various K-to-R mutations). We then examined the apical hook phenotype of all genotypes. The *HLS1pro:HA-HLS1* construct fully rescued the hookless phenotype of the *hls1-1* mutant (Fig. 4, A and B). However, expressing *HLS1* single-point mutants or *HLS1* variants carrying multiple mutations only partially rescued the hookless phenotype of *hls1-1*, while *HLS1pro:HA-HLS1*^{6KR} *hls1-1* had a more compromised apical hook curvature only slightly less pronounced than that of the *hls1-1* mutant (Fig. 4, A and B; Supplemental Fig. 4, A and B).

To further explore the genetic relationship between *HLS1* and *SIZ1* in regulating apical hook curvature, we generated the *siz1-2 hls1-1* double mutant by genetic crossing and *35S:SIZ1-GFP hls1-1* transgenic lines (*SIZ1OE hls1-1*, overexpressing *SIZ1* in *hls1-1*). We observed that *siz1-2 hls1-1* and *SIZ1OE hls1-1* dark-grown seedlings display the same hookless phenotype as *hls1-1* (Fig. 4, A and B; Supplemental Fig. 5, A and B), suggesting that *HLS1* acts genetically downstream of *SIZ1* in sustaining apical hook curvature.

SUMOylation regulates the function of its substrates by affecting protein stability, subcellular localization, enzymatic activity, and/or protein–protein interactions (Geoffroy and Hay 2009; Elrouby et al. 2013; Augustine and Vierstra 2018). To test whether HLS1 SUMOylation affects its protein stability, we performed cell-free degradation assays. Recombinant MBP-HLS1 was incubated with protein extracts from Col-0 or *siz1-2*. The results showed that HLS1 protein stability was not changed in *siz1-2*, indicating that SIZ1 does not affect HLS1 protein stability (Supplemental Fig. 6, A and B). We further tested HLS1 protein abundance in *HLS1OE*, *HLS1OE siz1-2*, and *HLS1*^{6KR}*OE* seedlings and determined that HLS1 levels do not change across these different

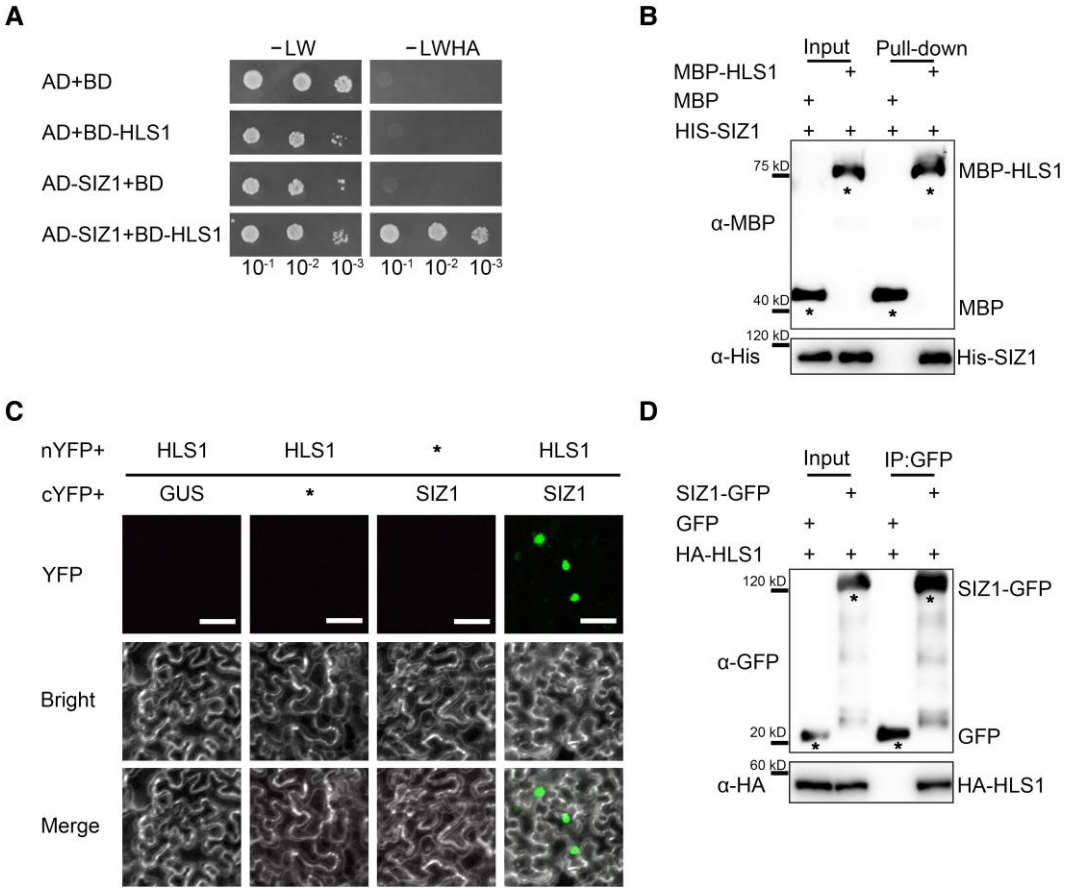

Figure 2. SIZ1 physically interacts with HLS1. **A)** Yeast 2-hybrid (Y2H) assays showing the interaction of SIZ1 with HLS1. Full-length SIZ1 was cloned into pGADT7 as prey (AD-SIZ1). Full-length HLS1 was cloned into pGBKT7 as bait (BD-HLS1). Each pair of bait and prey constructs was transformed into yeast strain AH109, grown on medium without Leu and Trp (-Leu/-Trp, -LW), and then screened on medium without Leu, Trp, His, or Ade (-LWHA). **B)** His pull-down assays detecting the interaction between SIZ1 and HLS1. An anti-MBP antibody was used to detect MBP-HLS1. The asterisks represent MBP or MBP-HLS1. **C)** SIZ1 interacts with HLS1, as determined by BiFC assays in *N. benthamiana*. Scale bars, 50 μm. **D)** Co-IP assays showing the interaction between SIZ1 and HLS1. Three-day-old dark-grown *HLS1pro:HA-FLAG-HLS1 SIZ1pro:SIZ1-GFP* and *HLS1pro:HA-FLAG-HLS1 SIZ1pro:GFP* transgenic seedlings were used for Co-IP assays. SIZ1 was detected with an anti-GFP antibody, and HA-HLS1 was detected with an anti-HA antibody. The asterisks represent GFP or GFP-SIZ1.

genotypes (Supplemental Fig. 6C). To investigate whether HLS1 SUMOylation might affect its subcellular localization, we transiently transfected the constructs *HLS1-GFP*, *HLS1^{6KR}-GFP*, and *MYC-SUMO1* as different combinations into Arabidopsis protoplasts isolated from Col-0, before visualizing the GFP signal using confocal microscopy. We detected green fluorescence from HLS1-GFP and HLS1^{6KR}-GFP in the nucleus, regardless of the co-transfection of *MYC-SUMO1* (Fig. 4C; Supplemental Fig. 7).

A recent study revealed that HLS1 self-association and oligomerization are required for its activation (Lyu et al. 2019). We thus asked whether HLS1 SUMOylation affects its potential for oligomerization by treating 3-d-old dark-grown seedlings with the chemical fixative paraformaldehyde (PFA). We observed a dramatic drop in the levels of oligomeric HLS1 in *HLS1^{6KR}OE hls1-1* and *HLS1OE siz1-2* when compared with that in *HLS1OE hls1-1* (Fig. 4D). Moreover, the levels of oligomeric HLS1 were similar in *HLS1^{6KR}OE hls1-1* and *HLS1OE siz1-2* seedlings (Fig. 4D). These results demonstrated that the differences in the oligomeric status of HLS1 in *HLS1OE hls1-1*, *HLS1^{6KR}OE hls1-1*, and *HLS1OE siz1-2* seedlings are due to the loss of SUMOylation rather than an effect of the introduced point mutations on protein structure. After light exposure, the abundance of oligomeric HLS1 decreased rapidly in all genotypes (Fig. 4D). In addition, light-inhibited HLS1 oligomerization was stronger in SUMOylation-defective *HLS1^{6KR}OE hls1-1* and *HLS1OE siz1-2* seedlings than in *HLS1OE hls1-1* (Fig. 4D). These results suggest that HLS1 SUMOylation is essential for its function in apical hook formation, and SUMOylated HLS1 is more likely to assemble into oligomers.

Light reduces HLS1 SUMOylation and oligomerization to initiate apical hook unfolding

Red light induces HLS1 de-oligomerization to initiate apical hook unfolding (Lyu et al. 2019). The above results indicated that SUMOylated HLS1 was more likely to assemble into

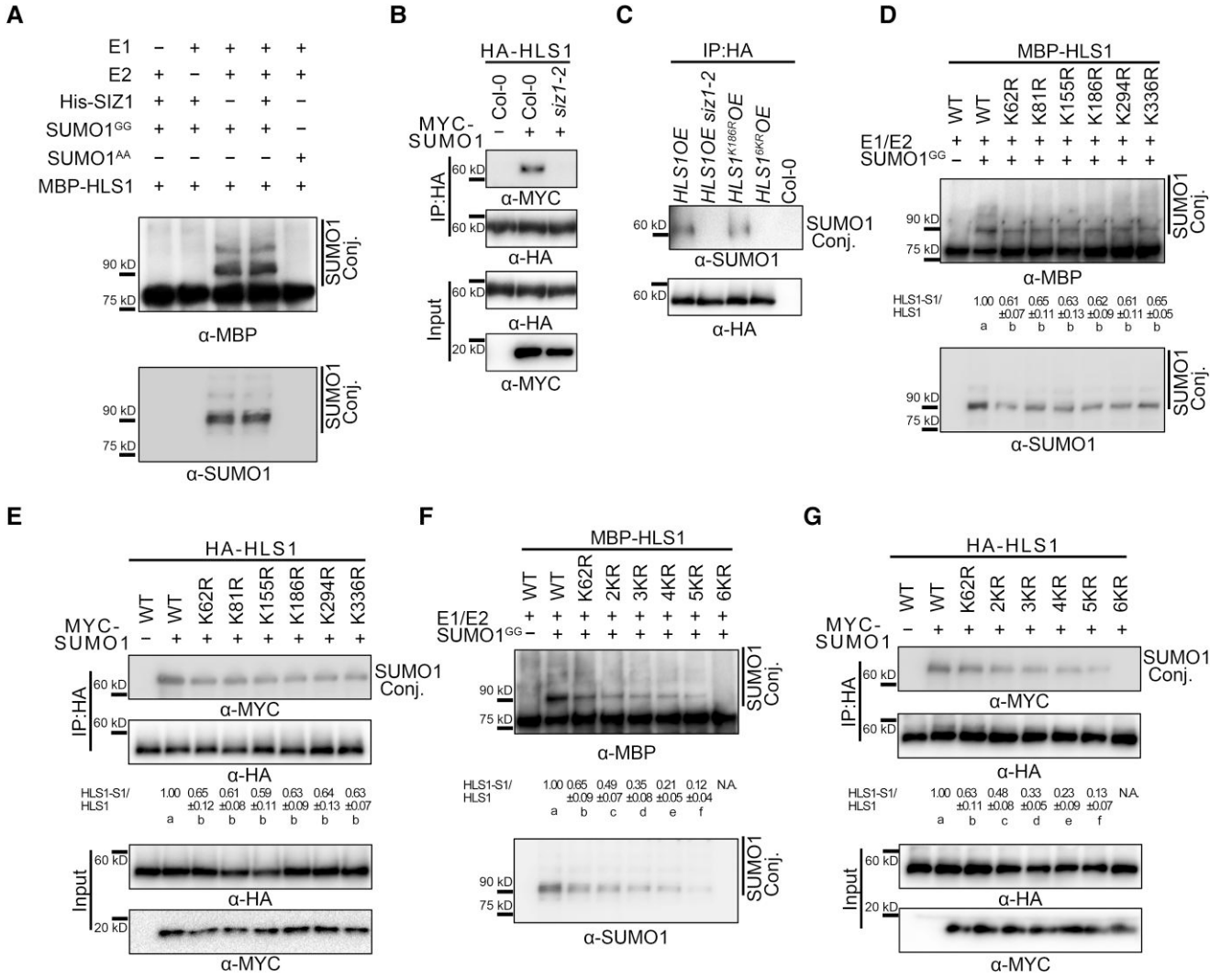

Figure 3. SIZ1 facilitates the SUMOylation of HLS1. **A)** In vitro SUMOylation assays showing the SUMOylation of HLS1. SUMOylated HLS1 was detected with anti-MBP and anti-SUMO1 antibodies. $SUMO1^{GG}$ and $SUMO1^{AA}$ represent the mature form of SUMO1 and the conjugation-deficient mutant of SUMO1, respectively. **B)** In vivo SUMOylation assays showing SIZ1-mediated HLS1 SUMOylation in vivo. *HA-HLS1* and *MYC-SUMO1* constructs were transiently transfected into Arabidopsis protoplasts prepared from Col-0 or *siz1-2*. Total proteins were extracted and then incubated with HA agarose beads. Anti-HA and anti-MYC antibodies were used to examine HLS1 SUMOylation. **C)** SUMOylation of HLS1 in *HLS1OE*, *HLS1OE siz1-2*, $HLS1^{K186R}OE$, and $HLS1^{6KR}OE$. Total proteins were extracted from 3-d-old dark-grown seedlings and then incubated with HA agarose beads. Anti-HA and anti-SUMO1 antibodies were used to examine HLS1 SUMOylation. **D)** In vitro SUMOylation assays showing the effects of point mutations of predicted SUMOylation sites on the SUMOylation of HLS1. *HA-HLS1* and *MYC-SUMO1* constructs were transiently transfected into Arabidopsis protoplasts prepared from Col-0. The SUMOylated HLS1(HLS1-S1)/HLS1 ratio was determined using ImageJ, with wild-type HLS1-S1 and HLS1 abundance set to 1. Data represent means ± SD from 3 independent experiments. Different lowercase letters indicate significant differences ($P < 0.05$) based on 1-way ANOVA followed by Fisher's LSD test. **E)** In vivo SUMOylation assays showing the effects of HLS1 point mutations on the SUMOylation of HLS1. *HA-HLS1* and *MYC-SUMO1* constructs were transiently transfected into Arabidopsis protoplasts prepared from Col-0. Total proteins were extracted and then incubated with HA agarose beads. Anti-HA and anti-MYC antibodies were used to examine HLS1 SUMOylation. **F)** In vitro SUMOylation assays showing the effects of HLS1 multiple mutations on the SUMOylation of HLS1. N.A., not available. **G)** In vivo SUMOylation assays showing the effects of HLS1 multiple mutations on the SUMOylation of HLS1. The SUMOylated HLS1(HLS1-S1)/HLS1 ratio was determined using ImageJ, with wild-type HLS1-S1 and HLS1 abundance set to 1. Data represent means ± SD from 3 independent experiments. Different lowercase letters indicate significant differences ($P < 0.05$) based on 1-way ANOVA followed by Fisher's LSD test.

oligomers than non-SUMOylated HSL1, which prompted us to hypothesize that light might suppress HLS1 SUMOylation. To test this hypothesis, we examined SUMOylated HLS1 levels in *HLS1OE hls1-1*, $HLS1^{6KR}OE$ *hls1-1*, and *HLS1OE siz1-2* dark-grown seedlings for up to 4 h after onset of light irradiation. As previously reported, HLS1 protein abundance did not appreciably change following the dark-to-light transition in *HLS1OE hls1-1* (Lyu et al. 2019) (Fig. 5A), as well as in $HLS1^{6KR}OE$ *hls1-1* and *HLS1OE siz1-2* (Fig. 5A). The levels of SUMOylated HLS1 gradually decreased with prolonged light

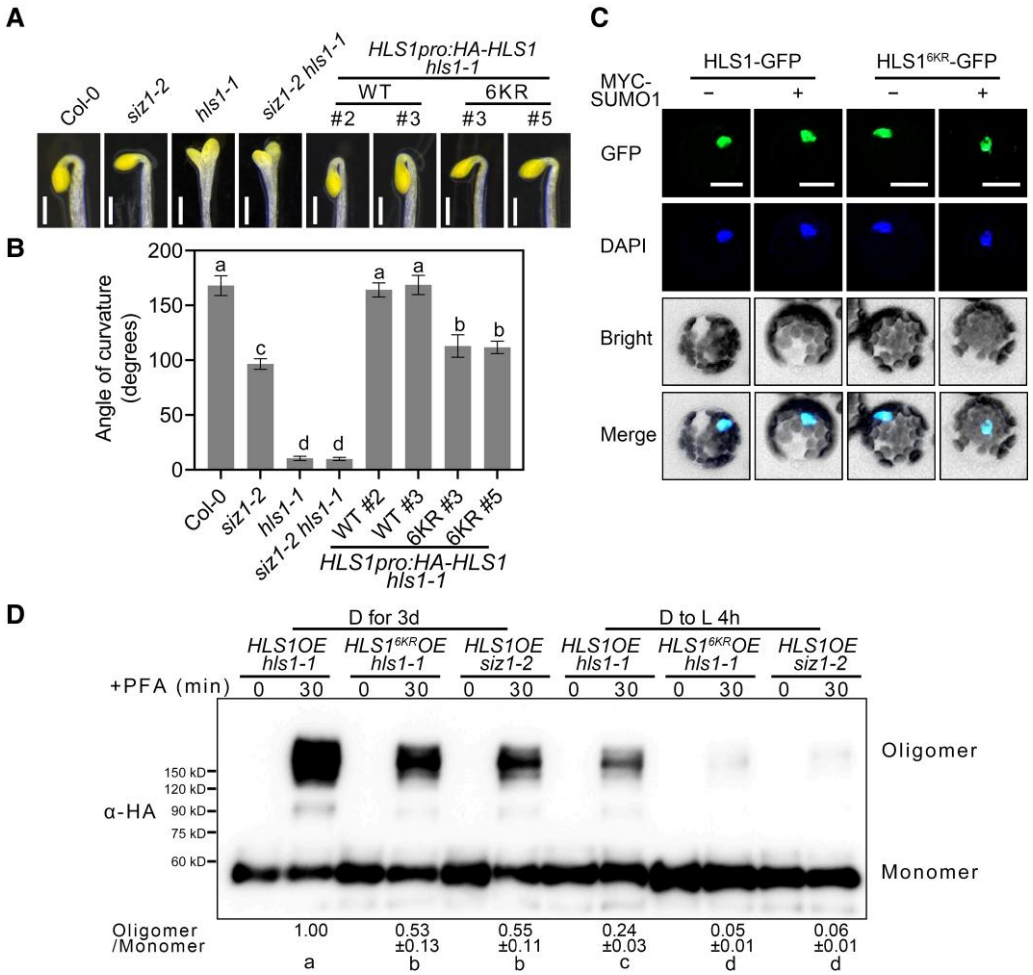

Figure 4. SUMOylation of HLS1 is required for its function. **A)** Apical hook phenotypes of 3-d-old dark-grown *siz1-2*, *siz1-2 hls1-1*, *HLS1pro:HA-HLS1 hls1-1*, and *HLS1pro:HA-HLS1^{6KR} hls1-1* seedlings. Scale bars, 1 mm. **B)** Quantification of apical hook curvature from seedlings shown in **A)**. Data represent means ± SE from 3 replicates, with each replicate consisting of at least 12 seedlings. Different lowercase letters indicate significant differences ($P < 0.05$) based on 1-way ANOVA followed by Fisher's LSD test. **C)** Subcellular localization of HLS1-GFP and HLS1^{6KR}-GFP. *HLS1-GFP* and *HLS1^{6KR}-GFP* constructs were transiently transfected into Arabidopsis protoplasts prepared from Col-0. The cell nucleus was labeled by DAPI staining. Scale bars, 20 μm. **D)** Chemical crosslinking assays showing the oligomerization status of HLS1 in *HLS1OE hls1-1*, *HLS1^{6KR}OE hls1-1*, and *HLS1OE siz1-2* seedlings. Seedlings were grown on half-strength MS medium in darkness for 3 d and then transferred to light (D to L) for 4 h. Seedlings were harvested and submerged in 0.5% (w/v) PFA solution for 30 min. An anti-HA antibody was used for immunoblotting. The oligomer/monomer ratio was determined using ImageJ, with oligomeric and monomeric HLS1 protein abundance in *HLS1OE hls1-1* set to 1. Data represent means ± SD from 3 independent experiments. Different lowercase letters indicate significant differences ($P < 0.05$) based on 1-way ANOVA followed by Fisher's LSD test.

exposure in *HLS1OE hls1-1*, whereas we failed to detect SUMOylated HLS1 in *HLS1^{6KR}OE/hls1-1* and *HLS1OE/siz1-2* (Fig. 5B). Reverse transcription quantitative PCR (RT-qPCR) and immunoblot analyses indicated that both *SIZ1* transcript levels and SIZ1 abundance decline in response to light (Fig. 5, C and D).

Since light-mediated inhibition of HLS1 oligomerization was stronger in SUMOylation-defective *HLS1^{6KR}OE hls1-1* and *HLS1OE siz1-2* (Fig. 4D), and as the photoreceptor phytochrome B (phyB) physically interacts with HLS1 to mediate its light-induced de-oligomerization (Lyu et al. 2019), we investigated whether HLS1 SUMOylation might affect the interaction of HLS1 with phyB. Accordingly, we performed Co-IP assays in Arabidopsis protoplasts co-transfected with relevant constructs using *MYC-SUMO1* to produce SUMOylated HLS1. We observed that SUMOylated HLS1 shows a weaker interaction with phyB than non-SUMOylated HLS1 (Fig. 5E).

We confirmed the effect of HLS1 SUMOylation on the HLS1–phyB interaction by transfecting protoplasts prepared from *HLS1OE* and *HLS1OE siz1-2* seedlings with the *phyB–GFP* construct. The HLS1–phyB interaction was enhanced in *HLS1OE siz1-2* protoplasts, indicating that SIZ1-mediated SUMOylation of HLS1 weakened the physical association between HLS1 and phyB (Fig. 5F). Furthermore, after being exposed to light, *HLS1pro:HA-HLS1^{6KR} hls1-1* seedlings showed a faster rate of apical hook opening than Col-0, while that of *HLS1pro:HA-HLS1 hls1-1* seedlings was comparable to Col-0 (Fig. 5, G and H). These results indicate that light-mediated

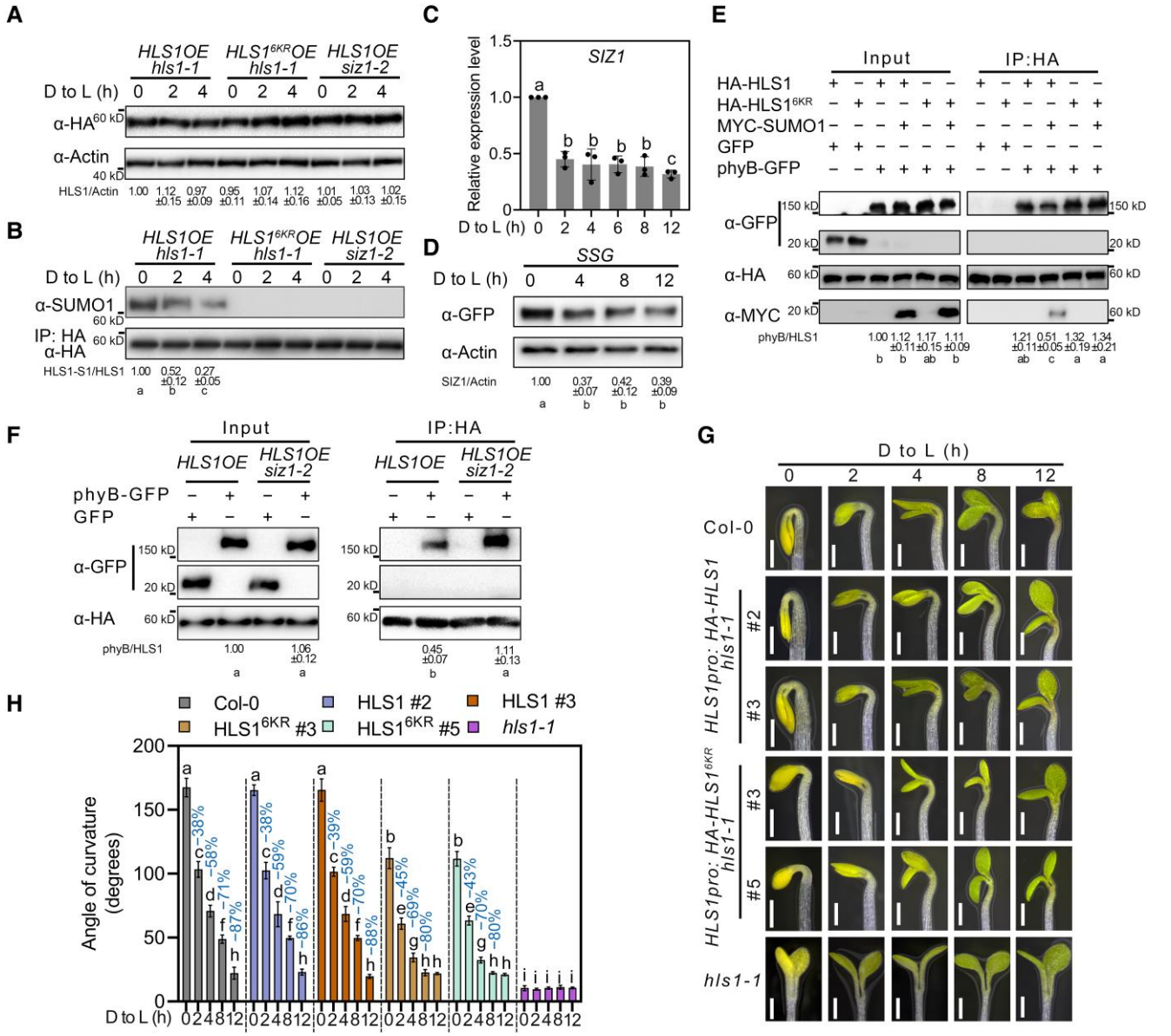

Figure 5. SUMOylation of HLS1 delays light-induced apical hook opening. **A)** HLS1 protein levels upon light exposure. Three-day-old dark-grown seedlings were transferred to light (D to L) for the indicated times. ACTIN served as a loading control. HLS1 abundance was determined using ImageJ, with HLS1 and ACTIN protein abundance of *HLS1OE hls1-1* in 0 h set to 1. Data represent means ± SD from 3 independent experiments. **B)** HLS1 SUMOylation upon light exposure. Total proteins were extracted and then incubated with HA agarose beads. Anti-SUMO1 was used to examine HLS1 SUMOylation. The SUMOylated HLS1 levels were determined using ImageJ, with SUMO-conjugated HLS1 and non-SUMOylated HLS1 protein abundance of *HLS1OE hls1-1* in darkness set to 1. Data represent means ± SD from 3 independent experiments. Different lowercase letters indicate significant differences ($P < 0.05$) based on 1-way ANOVA followed by Fisher's LSD test. **C)** Relative *SIZ1* transcript levels upon light exposure. *ACTIN2* expression was used as an internal reference. Data represent means ± SE from 3 replicates. Different lowercase letters indicate significant differences ($P < 0.05$) based on 1-way ANOVA followed by Fisher's LSD test. **D)** SIZ1 protein abundance upon light exposure. Three-day-old dark-grown *SSG* seedlings were transferred to light (D to L) for the indicated times. ACTIN served as a loading control. SIZ1 abundance was determined using ImageJ, with SIZ1 and ACTIN protein abundance before light exposure set to 1. Data represent means ± SD from 3 independent experiments. Different lowercase letters indicate significant differences ($P < 0.05$) based on 1-way ANOVA followed by Fisher's LSD test. **E)** Co-IP assays showing the effects of HLS1 SUMOylation on the HLS1–phyB interaction. *HA-HLS1*, *phyB–GFP*, and *MYC-SUMO1* constructs were transiently transfected into Arabidopsis protoplasts prepared from Col-0. Total proteins were extracted and then incubated with HA agarose beads. Anti-HA and anti-GFP antibodies were used for immunoblotting. The phyB/HLS1 ratio was determined using ImageJ, with HLS1 and phyB protein abundance in input set to 1. Data represent means ± SD from 3 independent experiments. Different lowercase letters indicate significant differences ($P < 0.05$) based on 1-way ANOVA followed by Fisher's LSD test. **F)** Co-IP assays showing the effects of SIZ1 on the HLS1–phyB interaction. The *phyB–GFP* construct was transiently transfected into Arabidopsis protoplasts prepared from *HLS1OE* or *HLS1OE siz1-2*. Total proteins were extracted and then incubated

(continued)

inhibition of SIZ1-catalyzed HLS1 SUMOylation, which enhances the interaction between phyB and HLS1 and decreases HLS1 oligomerization, is necessary to initiate apical hook opening.

HY5 suppresses SIZ1-mediated HLS1 SUMOylation to initiate apical hook unfolding

A recent study showed that *SIZ1* is a putative target of HY5 (Lee et al. 2007a). We therefore hypothesized that light suppresses *SIZ1* transcription via HY5. To test this hypothesis, we analyzed the promoter of *SIZ1* and identified 1 G-box, the cognate recognition site for HY5, and other basic leucine zipper (bZIP) transcription factors (Fig. 6A). Chromatin immunoprecipitation (ChIP)–qPCR assays indicated that HY5 binds to the fragment in the *SIZ1* promoter containing the G-box in planta (Fig. 6B). Subsequent electrophoretic mobility shift assays (EMSAs) determined that recombinant MBP-HY5 directly binds to the G-box of the *SIZ1* promoter (Fig. 6C).

To validate the HY5-mediated transcriptional inhibition of *SIZ1*, we performed luciferase reporter assays using the *SIZ1* promoter driving the firefly luciferase (*LUC*) reporter gene, while the effector construct consisted of *HY5* cloned in-frame and upstream of *GFP* (Fig. 6D). Co-transfecting the *SIZ1pro:LUC* reporter with *HY5-GFP* decreased *SIZ1* transcription, as evidenced by the lower relative LUC activity measured with HY5-GFP compared with no effector and the negative control *β-GLUCURONIDASE* (*GUS*)-*GFP* (Fig. 6E). We further examined relative *SIZ1* transcript levels in the *hy5* mutant and *HY5* overexpression transgenic line *35S:HY5-GFP* (*HY5OE*) for up to 12 h following the dark-to-light transition of etiolated seedlings. Compared with Col-0, *SIZ1* transcript levels were slightly higher in *hy5* but slightly lower in *HY5OE* in etiolated seedlings (Fig. 6F). Upon light exposure, *SIZ1* transcript levels decreased more sharply in *HY5OE* than in Col-0, while light did not alter *SIZ1* transcript levels in *hy5* (Fig. 6F). These results demonstrate that HY5 binds directly to the *SIZ1* promoter to suppress *SIZ1* transcription.

To further explore the association between HY5 and SIZ1 in apical hook development, we generated the *siz1-2 hy5* double mutant by genetic crossing. After transfer to light, *hy5* seedlings exhibited a delay in their apical hook opening, consistent with a previous study (Li and He 2016). Importantly, this phenotype was largely suppressed in the *siz1-2 hy5* double mutant (Fig. 7, A and B). We also measured the angle formed by the apical hook in etiolated *SIZ1OE* and *SIZ1OE hls1-1* seedlings exposed to light (Supplemental Fig. 5, A and B). Following the dark-to-light transition, we observed a delay in the opening of the apical hook in *SIZ1OE* similar to that in *hy5*, and *SIZ1OE hls1-1* showed the same hookless phenotype as *hls1-1* (Supplemental Fig. 5, A and B; Fig. 7, A and B).

Upon analyzing HLS1 abundance and SUMOylated HLS1 levels in *HLS1OE hls1-1* and *HLS1OE hls1-1 hy5* during the dark-to-light transition, we determined that the loss of HY5 function does not alter HLS1 protein abundance (Fig. 7C) but suppressed the light-induced decrease in SUMOylated HLS1 (Fig. 7D). HLS1 oligomeric levels in *HLS1OE hls1-1* and *HLS1OE hls1-1 hy5* were similar in the dark (Fig. 7E). After exposure to light for 4 h, the *HLS1OE hls1-1 hy5* mutant displayed a block in light-induced HLS1 de-oligomerization (Fig. 7E). These results indicate that HY5 suppresses *SIZ1* transcription, which leads to lower levels of HLS1 SUMOylation and oligomerization, thus initiating apical hook unfolding.

Discussion

Protein SUMOylation is induced by heat, ethanol treatment, drought, and oxidative stress (Saitoh and Hinchey 2000; Kurepa et al. 2003; Augustine et al. 2016). In addition to stress responses, protein SUMOylation is also involved in many basic cellular tasks. A previous study showed that SUMO target proteins participate in genome stability, cell cycle progression, chromatin maintenance and modification, transcription, translation, RNA splicing, and ribosome synthesis (Drabikowski et al. 2018). Proteomic studies have detected approximately 5,000 SUMO-modified proteins in Arabidopsis, suggesting that SUMOylation is as important as other post-translational modifications, such as phosphorylation and ubiquitination (Millar et al. 2019). SUMOylation is often compared with ubiquitination because of the similar catalytic steps responsible for their transfer onto substrate proteins (Kerscher et al. 2006). However, compared with the large number of ubiquitin E3 ligases, the Arabidopsis genome encodes only 2 SUMO E3 ligases, SIZ1 and HIGH PLOIDY2 (HPY2) (Morrell and Sadanandom 2019), indicating that each SUMO E3 ligase may be involved in multiple biological functions, each time serving as a hub to connect multiple signals. Therefore, it is necessary to identify and clarify each SUMO E3 ligase–mediated biological function. In this study, we provided evidence that SIZ1-meditated HLS1 SUMOylation plays a positive role in apical hook formation and revealed the dynamic changes in HLS1 SUMOylation during apical hook formation and light-induced apical hook unfolding.

Various environmental factors regulate plant growth, with light being arguably one of the most important, as it is an essential commodity for energy production via photosynthesis

Figure 5. (Continued)
with HA agarose beads. Anti-HA and anti-GFP antibodies were used for immunoblotting. **G)** Apical hook phenotypes of Col-0, *HLS1pro:HA-HLS1 hls1-1*, *HLS1pro:HA-HLS1^{6KR} hls1-1*, and *hls1-1* seedlings. Seedlings were grown on half-strength MS medium in darkness for 3 d and then transferred to light (D to L) for the indicated times. Scale bars, 1 mm. **H)** Quantification of apical hook curvature from seedlings shown in **G)**. Data represent means ± SE from 3 replicates, with each replicate consisting of at least 12 seedlings. Percentages represent the decrease in apical hook angle (light-induced angle/angle before light exposure). Different lowercase letters indicate significant differences ($P < 0.05$) based on 2-way ANOVA followed by Fisher's LSD test.

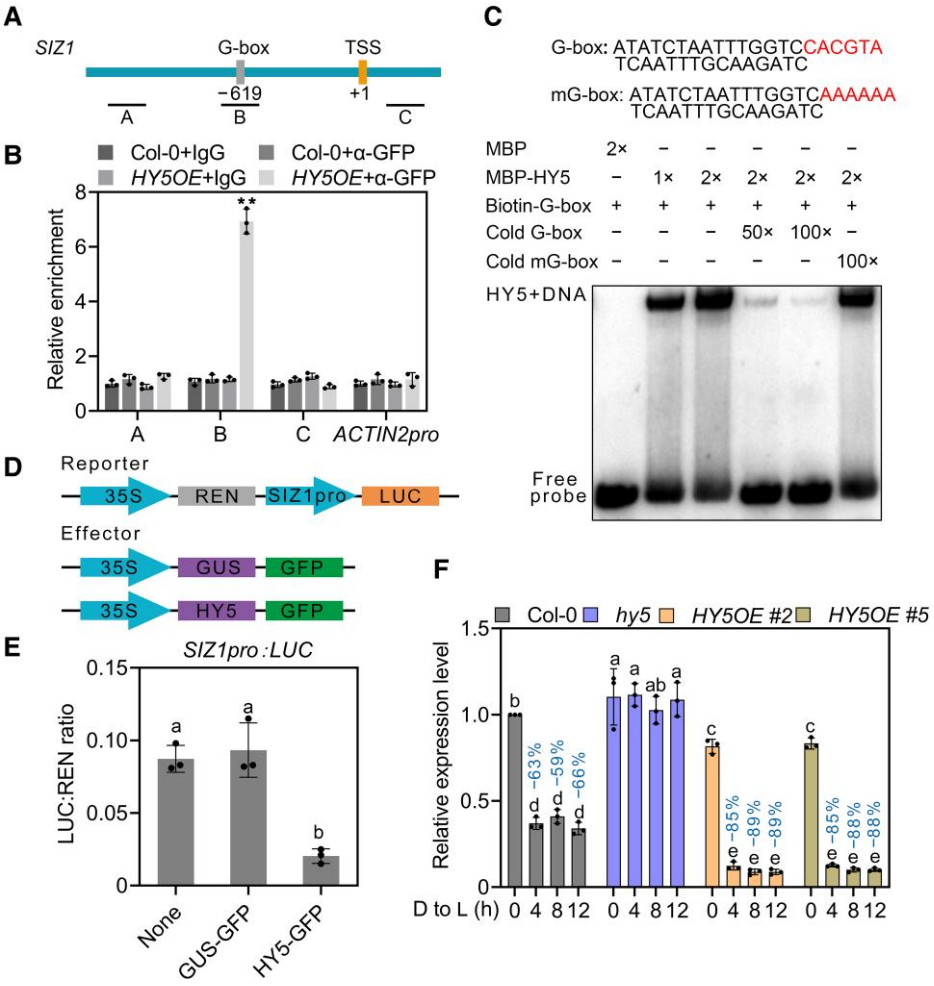

Figure 6. HY5 suppresses *SIZ1* transcription. **A)** Schematic diagram of the *SIZ1* promoter, with PCR amplicons indicated as letters A–C used for ChIP-qPCR. The positions of the transcription start site (TSS) and the G-box are indicated. **B)** ChIP-qPCR analysis of the enrichment of HY5 on *SIZ1* chromatin in Col-0 and *HY5*OE seedlings. Col-0 and IgG were used as negative controls, *TA3* was used for normalization, and *ACTIN2pro* was used as an internal control. Data represent means ± SE from 3 independent experiments; $^{**}P < 0.01$ based on Student's *t* test. **C)** EMSA showing that recombinant MBP-HY5 binds to the G-box of the *SIZ1* promoter in vitro. **D)** Schematic diagrams of the constructs used in the luciferase (LUC) reporter assays. **E)** Quantification of LUC activity. The *SIZ1pro:LUC* construct was co-transfected with *GUS-GFP* or *HY5-GFP* into Arabidopsis protoplasts prepared from Col-0. Data represent means ± SD from 3 independent experiments. Different lowercase letters indicate significant differences ($P < 0.05$) based on 1-way ANOVA followed by Fisher's LSD test. **F)** Relative *SIZ1* transcript levels in Col-0, *hy5*, and *HY5OE*. Seedlings were grown on half-strength MS medium in darkness for 3 d and then transferred to light (D to L) for the indicated times. Data represent means ± SE from 3 independent experiments. *ACTIN2* served as an internal control. Percentages represent the decrease in *SIZ1* transcript levels (light-induced transcript levels/transcript levels before light exposure). Different lowercase letters indicate significant differences ($P < 0.05$) based on 2-way ANOVA followed by Fisher's LSD test.

and an important signal that determines plant development hallmarks such as seed germination, seedling de-etiolation, organ development, flowering, and seed development (Gangappa and Botto 2016). Plants have evolved complex regulatory networks for photomorphogenesis, including by regulating chromatin structure, transcription rates, RNA processing, RNA methylation, RNA export, RNA degradation, translation, and post-translational modifications (Xu et al. 2015; Wang and Lin 2020). In this study, we demonstrate that HLS1 SUMOylation plays a positive role in apical hook development and provide a mechanism for photomorphogenesis (Fig. 8).

As a central regulator of apical hook formation, HLS1 function is regulated by various environmental stimuli and phytohormones. However, most of the regulation of HLS1 takes place at the transcriptional level (Wang and Guo 2019). For instance, *HLS1* transcription is directly regulated by the ethylene pathway transcription factors EIN3 and EIL1 (Li et al. 2004; An et al. 2012). GA, JA, and SA also regulate apical hook development via the EIN3/EIL1-*HLS1* signaling module and partly through the physical interaction of DELLA-EIN3, MYC2-EIN3, and NPR1-EIN3 (An et al. 2012; Song et al. 2014; Zhang et al. 2014, 2018; Huang et al. 2020). A bioinformatics prediction revealed that HLS1 displays sequence similarity to *N*-acetyltransferases

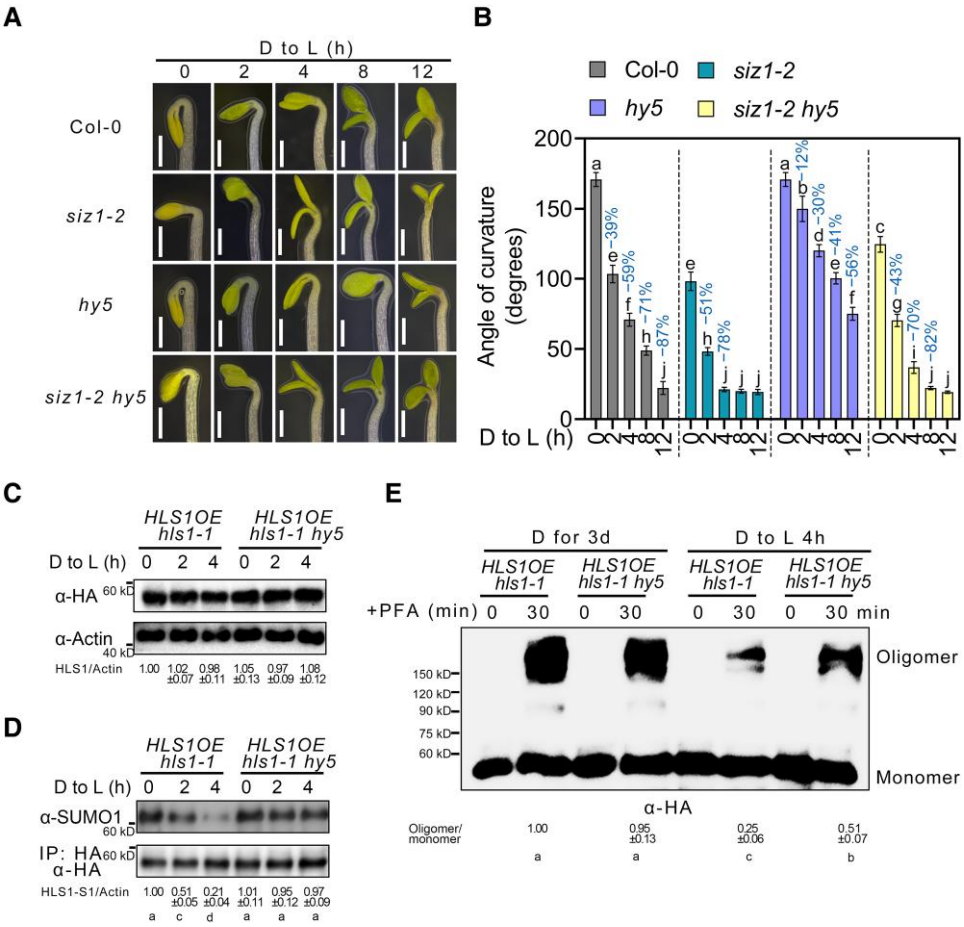

Figure 7. HY5 suppresses SIZ1-mediated HLS1 SUMOylation. **A)** Apical hook phenotypes of Col-0, *siz1-2*, *hy5*, and *siz1-2 hy5*. Seedlings were grown on half-strength MS medium in darkness for 3 d and then transferred to light (D to L) for the indicated times. Scale bars, 1 mm. **B)** Quantification of apical hook curvature from seedlings shown in **A)**. Data represent means ± SE from 3 replicates, with each replicate consisting of at least 12 seedlings. Percentages represent the change in the apical hook angle (light-induced angle/angle before light exposure). Different lowercase letters indicate significant differences ($P < 0.05$) based on 2-way ANOVA followed by Fisher's LSD test. **C)** HLS1 protein levels upon light exposure. Three-day-old dark-grown seedlings were transferred to light (D to L) for the indicated times. HLS1 was detected by immunoblotting with an HA antibody. ACTIN served as a loading control. HLS1 abundance was determined using ImageJ, with HLS1 and ACTIN protein abundance of *HLS1OE/hls1-1* in darkness set to 1. Data represent means ± SD from 3 independent experiments. Different lowercase letters indicate significant differences ($P < 0.05$) based on 1-way ANOVA followed by Fisher's LSD test. **D)** HLS1 SUMOylation upon light exposure. Total proteins were extracted and then incubated with HA agarose beads. Anti-HA and anti-SUMO1 antibodies were used to examine HLS1 SUMOylation. The SUMOylated HLS1 levels were determined using ImageJ, with SUMO-conjugated HLS1 and non-SUMOylated HLS1 protein abundance of *HLS1OE hls1-1* in darkness set to 1. **E)** Chemical crosslinking assays showing the oligomeric status of HLS1 in *HLS1OE hls1-1* and *HLS1OE hls1-1 hy5*. Three-day-old dark-grown seedlings were transferred to light (D to L) for 4 h. Seedlings were harvested and submerged in 0.5% (w/v) PFA solution for 30 min. An anti-HA antibody was used for immunoblotting. The oligomer/monomer ratio was determined using ImageJ, with oligomeric and monomeric HLS1 protein abundance in *HLS1OE hls1-1* set to 1. Data represent means ± SD from 3 independent experiments. Different lowercase letters indicate significant differences ($P < 0.05$) based on 1-way ANOVA followed by Fisher's LSD test.

(Lehman et al. 1996), and a recent study detected decreased levels of histone H3 acetylation at the *WRKY33* and *ABA INSENSITIVE5* (*ABI5*) loci in *hls1* mutants relative to the wild type (Liao et al. 2016). However, direct evidence for the *N*-acetyltransferase activity of HLS1, either in vivo or in vitro, is currently missing. The biochemical nature and mechanism of action of HLS1 thus remain enigmatic.

In this study, we discovered that HLS1 is post-translationally modified by SIZ1, resulting in the SUMOylation of HLS1, which is essential for its function in apical hook formation. Indeed, expressing wild-type *HLS1* in *hls1-1* under the *HLS1* promoter completely rescued the hookless phenotype of *hls1-1*, while expressing a version of *HLS1* that encodes a non-SUMOylated protein in the *hls1-1* background did so only partially. A previous study indicated that oligomerization is required for HLS1 activation (Lyu et al. 2019), and our study supports this idea. SUMOylated HLS1 is more likely to assemble into oligomers, whereas oligomeric forms of non-SUMOylated HLS proteins are much less abundant. We therefore propose that HLS1 SUMOylation in

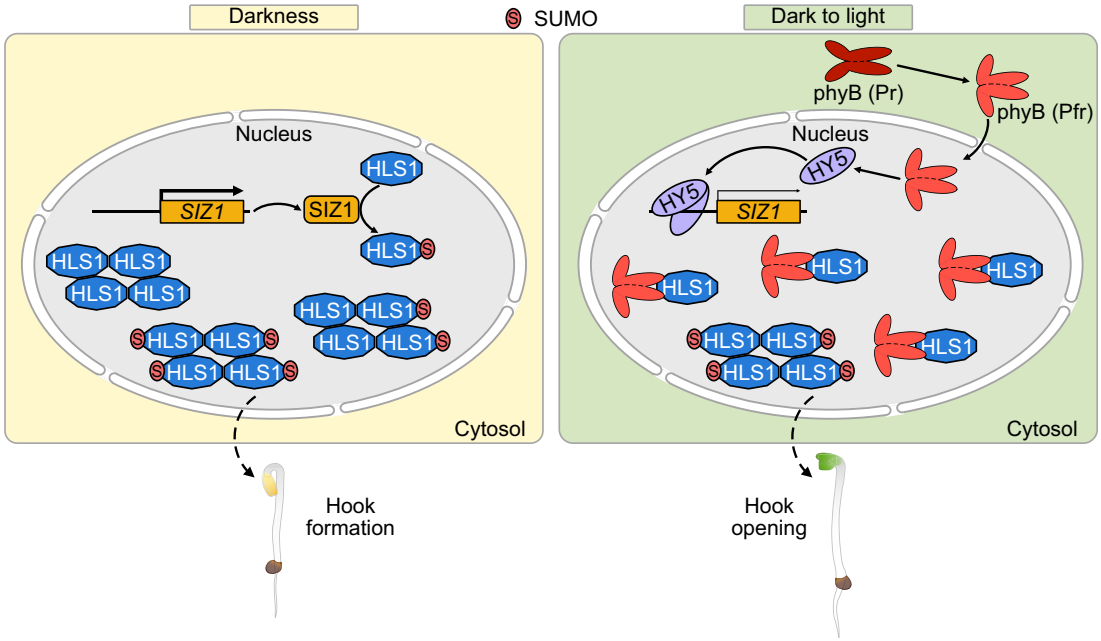

Figure 8. Proposed working model illustrating how HLS1 SUMOylation regulates apical hook development. SIZ1 induces the SUMOylation of HLS1 in darkness, and SUMOylated HLS1 assembles into oligomers to regulate apical hook formation. During the dark-to-light transition, light induces the translocation of phyB from the cytoplasm to the nucleus, where phyB interacts with HLS1 to suppress HLS1 oligomerization. In addition, HY5 suppresses *SIZ1* transcription to decrease HLS1 SUMOylation and oligomerization. Non-SUMOylated HLS1 displays a higher affinity for phyB, which also prevents HLS1 oligomerization. The decrease of oligomeric HLS1 leads to the deactivation of HLS1 and thus initiating apical hook unfolding.

darkness allows HLS1 to form active oligomeric forms more easily, thus improving its functional efficiency.

After reaching the soil surface, the next critical event for seedlings to survive is to undergo photomorphogenesis, which involves the quick disappearance of the apical hook, cotyledon opening, and chloroplast development (Kami et al. 2010). Light initiates apical hook opening during the dark-to-light transition, and *HLS1* transcript levels decrease after light exposure, although HLS1 protein remains stable during this time (Li et al. 2004; Lyu et al. 2019) (Fig. 5A). Moreover, light exposure does not affect the subcellular localization of HLS1 (Lyu et al. 2019), and HLS1 SUMOylation similarly did not change its protein abundance or nuclear localization, indicating that a change in HLS1 activity, rather than protein stability or subcellular localization, is the main mechanism behind the rapid apical hook opening in response to light. We showed that light suppressed *SIZ1* transcription to decrease the amount of SUMOylated HLS1, and *HLS1pro:HA-HLS1*^{6KR} *hls1-1* seedlings showed a faster rate of apical hook opening than *HLS1pro:HA-HLS1 hls1-1* during the dark-to-light transition, indicating that light reduces the extent of HLS1 SUMOylation to initiate apical hook unfolding.

SUMOylation-defective *HLS1*^{6KR} partially rescued the hookless phenotype of *hls1-1*, indicating that HLS1-mediated apical hook development is not entirely dependent on SIZ1-mediated SUMOylation. Moreover, the change in HLS1 oligomerization is a decisive factor in rapid apical hook opening in response to light. Previous studies revealed that oxidation/reduction of proteins plays critical roles in oligomerization (Tada et al. 2008; Tian et al. 2018; Lu et al. 2022); whether the same is true in HLS1 oligomerization remains unclear. Therefore, other HLS1 post-translational modifications should be further studied in response to light, as well as the effects of SUMOylation on other biochemical functions of HLS1. The *siz1-2* mutant showed a slightly more severe hook angle defect when compared to *HLS1pro:HA-HLS1*^{6KR} *hls1-1*, but the oligomeric status of HLS1 in *HLS1*^{6KR}*OE hls1-1* and *HLS1OE siz1-2* was almost the same, indicating that besides SIZ1-mediated HLS1 SUMOylation, other pathways likely contribute to SIZ1-modulated hook angle formation. A previous study detected more SA in *siz1-2* compared with the wild type (Lee et al. 2007b), and SA inhibits apical hook formation (Huang et al. 2020). The more pronounced loss of apical hook formation in *siz1-2* may therefore be caused by the combination of elevated SA levels and the loss of HLS1 SUMOylation. Indeed, the apical hook phenotype of *HLS1pro:HA-HLS1*^{6KR} *hls1-1* was almost the same as that of *NahG siz1-2*, in which SA no longer accumulates.

The perception of light by photoreceptors results in the regulation of many transcription factors (Gangappa and Botto 2016). HY5 has emerged as a central regulator of seedling development and promotes photomorphogenesis downstream of phytochromes, cryptochromes, and ultraviolet-B (UV-B) photoreceptors (Gangappa and Botto 2016). The loss of HY5 function did not alter the SUMOylation or oligomeric status of HLS1 in darkness, probably because HY5 protein abundance and activity are low in

the dark due to 26S proteasome–mediated degradation (Osterlund et al. 2000; Xu et al. 2015; Xiao et al. 2021). During the dark-to-light transition, light alleviates the inhibition of HY5 function caused by darkness. HY5 can then bind to the *SIZ1* promoter and suppress its transcription, which leads to lower HLS1 SUMOylation and oligomerization. The red light photoreceptor phyB physically interacts with HLS1 and mediates red light–induced de-oligomerization of HLS1 (Lyu et al. 2019). Combined with our previous results, this study elaborates on the mechanism by which the apical hook rapidly unfolds under different light qualities. Interestingly, HLS1 SUMOylation weakened the physical association of HLS1 and phyB. We thus propose that light quickly initiates apical hook opening, as outlined in Fig. 8. In response to light, HY5 suppresses *SIZ1* transcription, which leads to de-SUMOylation of HLS1. On the one hand, non-SUMOylated HLS1 is more difficult to assemble into oligomers. On the other hand, non-SUMOylated HLS1 displays a higher affinity to phyB, which also prevents HLS1 oligomerization. SIZ1-mediated HLS1 SUMOylation therefore broadens our understanding of quick apical hook opening in response to light.

Materials and methods

Plant materials and growth conditions

The wild-type Arabidopsis (*A. thaliana*) seeds used in this study were Col-0. The *siz1-2* (SALK_065397) and *hy5* (SALK_096651) mutants were obtained from the Arabidopsis Biological Resource Center (ABRC), and the details have been described before (Jin et al. 2008; Yang et al. 2018). The *SSG*, *NahG*, and *NahG siz1-2* seeds were obtained from Prof. Jingbo Jin (Chinese Academy of Sciences) and have been described by Jin et al. (2008). The *hls1-1* was obtained from Prof. Fei Yu (Northwest A&F University) and has been described before (Guzman and Ecker 1990). Arabidopsis seeds used in the study were sterilized using 70% (v/v) ethanol and 0.1% (v/v) Triton X-100 and plated on half-strength Murashige and Skoog (MS) medium and stratified at 4 °C for 2 d in the darkness. Seeds were then incubated for 6 h in light (150 μmol m^{-2} s^{-1}, 16-W T8-type LED) at 22 °C for germination and then grown under a long-day condition (22 °C, light 16 h/dark 8 h). *N. benthamiana* plants were grown on soil (Pindstrup substrate 0–6 mm, pH 6.0) under a long-day condition (150 μmol m^{-2} s^{-1}, 25 °C, light 16 h/dark 8 h). Four-week-old soil-grown *N. benthamiana* plants were used in all experiments. The primers used for genotyping are listed in Supplemental Data Set 1.

For phenotypic observation, seeds exposed to light for 6 h to induce germination were then grown in the darkness for 3 d. The apical hooks were imaged and the curvature was measured using ImageJ software (https://imagej.nih.gov/ij/).

Y2H assays

A Seamless Cloning and Assembly Kit (Vazyme) was used for the plasmid constructions. For Y2H screen, full-length *SIZ1* was cloned into the pGBKT7 (Clontech) vector to generate a bait vector with SIZ1 to the GAL4 DNA-binding domain. The bait construct was further co-transformed into the yeast strain AH109 with a prey cDNA library generated from 3-d-old dark-grown Arabidopsis seedlings, which was constructed by fusing cDNAs with the GAL4 activation domain in the pGADT7 vector. The transformants were screened on the Quadruple DO supplement (-Leu/-Trp/-His/-Ade, -LWHA). Positive clones were isolated, and their self-activation activities were checked by co-transformation with an empty pGADT7 (Clontech) vector. Those positive clones without self-activation activities were further identified by sequence (Zhang et al. 2021). For Y2H assays, full-length *SIZ1* was cloned into pGADT7 as prey. Full-length *HLS1* was cloned into pGBKT7 as bait. Each pair of bait and prey constructs was transformed into yeast strain AH109, grown on Double DO supplement (-Leu/-Trp, -LW) for 3 d, and transferred onto Quadruple DO supplement to test possible interaction (Zhang et al. 2021). The procedure is detailed in the Make Your Own "Mate & Plate" Library System User Manual and Yeast Two-Hybrid System User Manual (Clontech). The primers used for plasmid construction are listed in Supplemental Data Set 1.

In vitro pull-down assays

In vitro pull-down assays were performed as described previously (Zhang et al. 2021). Full-length *HLS1* and *SIZ1* were cloned into pMAL-c2x (MBP tag) and pET-28a (+) vector (His tag), respectively (Zhang et al. 2021). MBP-HLS1 was purified using amylose resin (NEB), and His-SIZ1 was purified using NiNTA agarose (Invitrogen). Purified MBP or MBP-HLS1 beads were incubated with equal amounts of His-SIZ1 in MBP pull-down binding buffer (20 mM Tris-HCl, pH 7.5, 100 mM NaCl, 1 mM EDTA) at 4 °C for 2 h. After washing 7 times with MBP pull-down washing buffer [200 mM NaCl, 1 mM EDTA, 0.5% (v/v) Nonidet P-40, 20 mM Tris-HCl, pH 8.0], the beads were collected, boiled in 50 μL 2× SDS loading buffer for 8 min at 100 °C, and the sample examined by immunoblotting using anti-His (1:5,000 dilution, ABclonal, China, AE003) and anti-MBP (1:5,000 dilution, ABclonal, China, AE016) antibodies. The primers used for plasmid construction are listed in Supplemental Data Set 1.

BiFC assays

Full-length *HLS1* was cloned into pXY103 vector carrying the N-terminal fragment of YFP, and *SIZ1* was cloned into pXY104 vector carrying the C-terminal fragment of YFP (Yu et al. 2008). *Agrobacterium tumefaciens* strain GV3101 was transformed with the above vector or control vector [β-GLUCURONIDASE (GUS)-pXY104, empty pXY103, or empty pXY104]. Agrobacterium cultures were grown overnight in LB medium containing 200 mM acetosyringone, washed with infiltration medium (10 mM $MgCl_2$, 10 mM MES, pH 5.7, 200 mM acetosyringone) and resuspended to an OD_{600} of 1.0. Agrobacterium carrying nYFP and cYFP constructs was mixed in equal ratios, and the Agrobacterium

mixtures were infiltrated into the young leaves of *N. benthamiana*. After 36 to 48 h, YFP was excited with a 514 nm laser line (5× intensity) and detected from 530 to 560 nm (2.5× gains). YFP signals were detected using a fluorescence microscope (Leica) (Yu et al. 2008). The primers used for plasmid construction are listed in Supplemental Data Set 1.

Co-IP assays

For SIZ1–HLS1 interaction, 3-d-old dark-grown *HLS1pro:HA-FLAG-HLS1 SIZ1pro:SIZ1-GFP* and *HLS1pro:HA-FLAG-HLS1 SIZ1pro:GFP* transgenic seedlings were used for Co-IP assays (Zhang et al. 2021). The total proteins were extracted from different seedlings and then incubated with GFP agarose beads (Chromotek) in IP buffer [10 mM Tris-HCl, pH 7.5, 0.5% (v/v) Nonidet P-40, 2 mM EDTA, 150 mM NaCl, 1 mM PMSF, and 1% (w/v) protease inhibitor]. The beads were collected and washed at least 5 times with IP buffer, then the interaction by immunoblotting was examined using anti-HA (1:5,000 dilution, Sigma-Aldrich, USA, H6908) and anti-GFP (1:5,000 dilution, Transgen, China, HT801) antibodies. For HLS1–phyB interaction, *HA-HLS1*, *MYC-SUMO1*, *GFP*, and *phyB–GFP* plasmids were transformed into Arabidopsis protoplasts isolated from Col-0 or *siz1-2*. Arabidopsis protoplasts were prepared as described previously (Yoo et al. 2007). After 16 h of expression in the darkness, protoplasts were transferred to light for 2 h, and then proteins were extracted and incubated with HA agarose beads in IP buffer. The anti-HA, anti-MYC (1:5,000 dilution, Cwbio, China, cw0299M), and anti-GFP antibodies were used for immunoblotting. The antibody source details are listed in Supplemental Table 1.

Plant transformation

Full-length *HLS1* was cloned into pCM1307 plasmid to construct *35S:HA-FLAG-HLS1*. For *HLS1pro:HA-FLAG-HLS1*, *35S* promoter in *35S:HA-FLAG-HLS1* was replaced by *HLS1* promoter (Zhang et al. 2021). All these constructs were introduced into *A. tumefaciens* strain GV3101 and transformed into Arabidopsis plants using the floral dip method described previously (Zhang et al. 2006). The primers used for plasmid construction are listed in Supplemental Data Set 1.

In vitro SUMOylation assays

The in vitro SUMOylation assays were performed as described previously (Lin et al. 2016; Zhang et al. 2019; Zheng et al. 2020). His-SUMO1^{GG} (the mature form of SUMO1, with the C-terminal double-Gly motif exposed) and His-SUMO1^{AA} (a conjugation-defective SUMO1 mutant, with the double-Gly motif mutated to double-Ala) were used in the in vitro SUMOylation assays. In brief, 30 μL reaction buffer (200 mM HEPES, pH 7.5, 5 mM $MgCl_2$, and 2 mM ATP) contains 50 ng of His-SAE1b, 50 ng of His-SAE2, 50 ng of His-SCE1, 8 μg of His-SUMO1^{GG} or His-SUMO1^{AA}, and 100 ng of MBP-HLS1. After incubation for 3 h at 30 °C, the reaction was stopped by adding 5× SDS loading buffer. SUMOylated MBP-HLS1 was analyzed by immunoblotting with anti-MBP and anti-SUMO1 (1:5,000 dilution, Abcam, UK, ab5316) antibodies. Details on antibodies are provided in Supplemental Table 1.

In vivo SUMOylation assays

The in vivo SUMOylation assays were performed as described previously (Niu et al. 2019; Zheng et al. 2020) with some modifications. Briefly, full-length *SUMO1* was cloned into pCM1307 plasmid to construct *35S:MYC-SUMO1* (Zhang et al. 2021). The *HA-HLS1* and *MYC-SUMO1* plasmids were transformed into Arabidopsis protoplasts isolated from Col-0 or *siz1-2*. After 16 h of expression in the darkness, proteins were extracted and incubated with HA agarose beads in IP buffer, then detected the SUMOylation by immunoblotting using anti-HA and anti-MYC antibodies.

Subcellular localization

The *HLS1-GFP* and *MYC-SUMO1* were transformed into Arabidopsis protoplasts isolated from Col-0. After 16 h of expression in the darkness, the GFP signal was observed using a Zeiss confocal microscope (Cell Observer SD), and GFP was excited with a 488 nm laser line (50% intensity) and detected from 495 to 550 nm (20× objective). The cell nucleus was revealed by 4,6-diamidino-2-phenylindole (DAPI) staining, and DAPI was excited with a 360 nm laser line (50% intensity) and detected from 435 to 485 nm (20× objective). MYC-SUMO1 was confirmed by immunoblotting with anti-MYC and anti-ACTIN (1:10,000 dilution, Cwbio, China, cw0264A) antibodies.

Chemical crosslinking

Chemical crosslinking was performed as described previously (Lyu et al. 2019; Wu et al. 2020). Three-day-old dark-grown seedlings were harvested and submerged in 0.5% PFA (w/v) solution for 30 min. An anti-HA antibody was used for the immunoblotting analysis.

RNA extraction and RT-qPCR

Total RNA was extracted by Total RNA Extraction Kit (Solarbio). For RT-qPCR, cDNA was prepared using PrimeScript RT reagent Kit (Takara). Gene expression was detected and analyzed using SYBR Green PCR Master Mix (Invitrogen) and the CFX Connect Real-Time System (Bio-Rad). For each sample, 3 replicates were performed, and the expression was normalized to *ACTIN2*. The primers used for RT-qPCR are listed in Supplemental Data Set 1.

Electrophoretic mobility shift assays

DNA–protein binding reaction and detection were accomplished using a Chemiluminescent EMSA Kit (Beyotime). The DNA probe (see Supplemental Data Set 1) labeled by biotin was incubated with MBP-HY5 or MBP in EMSA binding buffer (25 mM HEPES-KOH, pH 8.0, 50 mM KCl, 1 mM DTT, and 10% glycerol), the nonlabeled DNA probe was used as a competitor, and the nonlabeled mutated DNA probe was used as a negative control. The resulting products were then subjected to native polyacrylamide gel

electrophoresis, followed by transfer to a nylon membrane, which was used for detection of EMSA signals according to the manufacturer's instructions.

ChIP-qPCR assays

ChIP was performed as previously described (Zheng et al. 2019). Briefly, 3-d-old dark-grown *HY5OE* seedlings were transferred to light for 4 h, and then 2 g seedlings were harvested and crosslinked with formaldehyde and used for chromatin isolation. The chromatin was sonicated 5 times (15 s on and 15 s off) on ice and immunoprecipitated using 20 μL anti-GFP or IgG antibody. Immunoprecipitated proteins were collected with 40 μL protein A beads. After reverse crosslinking, the DNA fragments were quantified by qPCR using specific primer sets (Supplemental Data Set 1). Col-0 and IgG were used as negative controls, *TA3* was used for normalization, and *ACTIN2pro* served as an internal control. Three biological replicates were carried out.

Statistical analysis

The experimental data were statistically analyzed using 3 or more averages. The significance of the differences between groups was determined by a 2-tailed Student's *t* test, $^{*}P < 0.05$ and $^{**}P < 0.01$. For multiple comparisons, using 1-way or 2-way ANOVA, it was considered significant when $P < 0.05$. Statistical data are provided in Supplemental Data Set 2.

Accession numbers

The accession numbers of the main genes discussed in this article are SIZ1 (AT5G60410), HLS1 (AT4G37580), SUMO1 (AT4G26840), HY5 (AT5G11260), phyB (AT2G18790), and ACTIN2 (AT3G18780).

Acknowledgments

We thank Prof. Jingbo Jin (Chinese Academy of Sciences) for providing *SSG*, *NahG*, and *NahG siz1-2* seeds, Prof. Fei Yu (Northwest A&F University) for providing *hls1-1* seeds, and Prof. Shangwei Zhong (Peking University) for his technical help with the chemical crosslinking.

Author Contributions

D.Z.: conceptualization; F.W. and F.Y.: methodology; J.X., F.Y., and F.W.: investigation; J.X. and D.Z.: visualization; H.L. and D.Z.: supervision; J.X.: writing—original draft; D.Z.: writing—review and editing.

Supplemental data

The following materials are available in the online version of this article.

Supplemental Figure S1. Dynamic apical hook formation after seed germination.

Supplemental Figure S2. The elevated SA levels in *siz1-2* do not contribute much to the hook-deficient phenotype.

Supplemental Figure S3. Potential SUMOylation sites in HLS1.

Supplemental Figure S4. Apical hook phenotypes and curvature of different genotypes.

Supplemental Figure S5. HLS1 acts genetically downstream of SIZ1 in sustaining apical hook curvature.

Supplemental Figure S6. HLS1 SUMOylation does not affect HLS1 protein stability.

Supplemental Figure S7. Confirmation of MYC-SUMO1 accumulation in the subcellular localization analysis.

Supplemental Table S1. Key resources.

Supplemental Data Set 1. The primers used in this study.

Supplemental Data Set 2. ANOVA results.

Funding

This work was supported by grants from National Natural Science Foundation of China (32070213 and 32270258); Sichuan Science and Technology Program (2022JDRC0032); Institutional Research Fund of Sichuan University (2020SCUNL212); Fundamental Research Funds for the Central Universities (SCU2020D003); and Sichuan Forage Innovation Team Program.

Conflict of interest statement. None declared.

References

An F, Zhang X, Zhu Z, Ji Y, He W, Jiang Z, Li M, Guo H. Coordinated regulation of apical hook development by gibberellins and ethylene in etiolated Arabidopsis seedlings. Cell Res. 2012:**22**(5):915–927. https://doi.org/10.1038/cr.2012.29

Augustine RC, Vierstra RD. SUMOylation: re-wiring the plant nucleus during stress and development. Curr Opin Plant Biol. 2018:**45**(Pt A): 143–154. https://doi.org/10.1016/j.pbi.2018.06.006

Augustine RC, York SL, Rytz TC, Vierstra RD. Defining the SUMO system in maize: SUMOylation is up-regulated during endosperm development and rapidly induced by stress. Plant Physiol. 2016:**171**(3): 2191–2210. https://doi.org/10.1104/pp.16.00353

Bernula P, Pettko-Szandtner A, Hajdu A, Kozma-Bognar L, Josse E-M, Adam E, Nagy F, Viczian A. SUMOylation of PHYTOCHROME INTERACTING FACTOR 3 promotes photomorphogenesis in Arabidopsis thaliana. New Phytol. 2020:**229**(4): 2050–2061. https://doi.org/10.1111/nph.17013

Béziat C, Barbez E, Feraru MI, Lucyshyn D, Kleine-Vehn J. Light triggers PILS-dependent reduction in nuclear auxin signalling for growth transition. Nat Plants. 2017:**3**(8):17105. https://doi.org/10.1038/nplants.2017.105

Beziat C, Kleine-Vehn J. The road to auxin-dependent growth repression and promotion in apical hooks. Curr Biol. 2018:**28**(8): R519–R525. https://doi.org/10.1016/j.cub.2018.01.069

Creton S, Jentsch S. Snapshot: the SUMO system. Cell. 2010:**143**(5): 848. https://doi.org/10.1016/j.cell.2010.11.026

Drabikowski K, Ferralli J, Kistowski M, Oledzki J, Dadlez M, Chiquet-Ehrismann R. Comprehensive list of SUMO targets in Caenorhabditis elegans and its implication for evolutionary conservation of SUMO signaling. Sci Rep. 2018:**8**(1):1139. https://doi.org/10.1038/s41598-018-19424-9

Du M, Daher FB, Liu Y, Steward A, Tillmann M, Zhang X, Wong JH, Ren H, Cohen JD, Li C, et al. Biphasic control of cell expansion by auxin coordinates etiolated seedling development. Sci Adv. 2022:**8**(2):eabj1570. https://doi.org/10.1126/sciadv.abj1570

Elrouby N, Bonequi MV, Porri A, Coupland G. Identification of Arabidopsis SUMO-interacting proteins that regulate chromatin activity and developmental transitions. Proc. Natl Acad Sci U S A. 2013:**110**-(49):19956–19961. https://doi.org/10.1073/pnas.1319985110

Gangappa SN, Botto JF. The multifaceted roles of HY5 in plant growth and development. Mol Plant. 2016:**9**(10):1353–1365. https://doi.org/10.1016/j.molp.2016.07.002

Geoffroy MC, Hay RT. An additional role for SUMO in ubiquitin-mediated proteolysis. Nat Rev Mol Cell Biol. 2009:**10**(8):564–568. https://doi.org/10.1038/nrm2707

Gou M, Huang Q, Qian W, Zhang Z, Jia Z, Hua J. Sumoylation E3 ligase SIZ1 modulates plant immunity partly through the immune receptor gene SNC1 in Arabidopsis. Mol Plant-Microbe Interact. 2017:**30**(4):334–342. https://doi.org/10.1094/MPMI-02-17-0041-R

Guzman P, Ecker JR. Exploiting the triple response of Arabidopsis to identify ethylene-related mutants. Plant Cell. 1990:**2**(6):513–523. https://doi.org/10.1105/tpc.2.6.513

Huang P, Dong Z, Guo P, Zhang X, Qiu Y, Li B, Wang Y, Guo H. Salicylic acid suppresses apical hook formation via NPR1-mediated repression of EIN3 and EIL1 in Arabidopsis. Plant Cell. 2020:**32**(3):612–629. https://doi.org/10.1105/tpc.19.00658

Jin JB, Jin YH, Lee J, Miura K, Yoo CY, Kim WY, Van Oosten M, Hyun Y, Somers DE, Lee I, et al. The SUMO E3 ligase, AtSIZ1, regulates flowering by controlling a salicylic acid-mediated floral promotion pathway and through affects on FLC chromatin structure. Plant J. 2008:**53**(3):530–540. https://doi.org/10.1111/j.1365-313X.2007.03359.x

Kami C, Lorrain S, Hornitschek P, Fankhauser C. Light-regulated plant growth and development. Curr Top Dev Biol. 2010:**91**:29–66. https://doi.org/10.1016/S0070-2153(10)91002-8

Kerscher O, Felberbaum R, Hochstrasser M. Modification of proteins by ubiquitin and ubiquitin-like proteins. Annu Rev Cell Dev Biol. 2006:**22**(1):159–180. https://doi.org/10.1146/annurev.cellbio.22.010605.093503

Kim S-I, Park BS, Kim DY, Yeu SY, Song SI, Song JT, Seo HS. E3 SUMO ligase AtSIZ1 positively regulates SLY1-mediated GA signalling and plant development. Biochem J. 2015:**469**(2):299–314. https://doi.org/10.1042/BJ20141302

Kong X, Hong Y, Hsu YF, Huang H, Liu X, Song Z, Zhu JK. SIZ1-mediated SUMOylation of ROS1 enhances its stability and positively regulates active DNA demethylation in Arabidopsis. Mol Plant. 2020:**13**(12):1816–1824. https://doi.org/10.1016/j.molp.2020.09.010

Kurepa J, Walker JM, Smalle J, Gosink MM, Davis SJ, Durham TL, Sung D-Y, Vierstra RD. The small ubiquitin-like modifier (SUMO) protein modification system in Arabidopsis: accumulation of SUMO1 and-2 conjugates is increased by stress. J Biol Chem. 2003:**278**(9):6862–6872. https://doi.org/10.1074/jbc.M209694200

Lee J, He K, Stolc V, Lee H, Figueroa P, Gao Y, Tongprasit W, Zhao H, Lee I, Deng XW. Analysis of transcription factor HY5 genomic binding sites revealed its hierarchical role in light regulation of development. Plant Cell. 2007a:**19**(3):731–749. https://doi.org/10.1105/tpc.106.047688

Lee J, Nam J, Park HC, Na G, Miura K, Jin JB, Yoo CY, Baek D, Kim DH, Jeong JC, et al. Salicylic acid-mediated innate immunity in Arabidopsis is regulated by SIZ1 SUMO E3 ligase. Plant J. 2007b:**49**(1):79–90. https://doi.org/10.1111/j.1365-313X.2006.02947.x

Lehman A, Black R, Ecker JR. HOOKLESS1, an ethylene response gene, is required for differential cell elongation in the Arabidopsis hypocotyl. Cell. 1996:**85**(2):183–194. https://doi.org/10.1016/S0092-8674(00)81095-8

Li H, Johnson P, Stepanova A, Alonso JM, Ecker JR. Convergence of signaling of differential cell growth pathways in the control in Arabidopsis. Dev Cell. 2004:**7**(2):193–204. https://doi.org/10.1016/j.devcel.2004.07.002

Li QF, He JX. BZR1 interacts with HY5 to mediate brassinosteroid- and light-regulated cotyledon opening in Arabidopsis in darkness. Mol Plant. 2016:**9**(1):113–125. https://doi.org/10.1016/j.molp.2015.08.014

Liao C-J, Lai Z, Lee S, Yun D-J, Mengiste T. Arabidopsis HOOKLESS1 regulates responses to pathogens and abscisic acid through interaction with MED18 and acetylation of WRKY33 and ABI5 chromatin. Plant Cell. 2016:**28**(7):1662–1681. https://doi.org/10.1105/tpc.16.00105

Lin X-L, Niu D, Hu Z-L, Kim DH, Jin YH, Cai B, Liu P, Miura K, Yun D-J, Kim W-Y, et al. An Arabidopsis SUMO E3 ligase, SIZ1, negatively regulates photomorphogenesis by promoting COP1 activity. PLoS Genet. 2016:**12**(4):e1006016. https://doi.org/10.1371/journal.pgen.1006016

Lu Q, Houbaert A, Ma Q, Huang J, Sterck L, Zhang C, Benjamins R, Coppens F, Van Breusegem F, Russinova E. Adenosine monophosphate deaminase modulates BIN2 activity through hydrogen peroxide-induced oligomerization. Plant Cell. 2022:**34**(10):3844–3859. https://doi.org/10.1093/plcell/koac203

Lyu M, Shi H, Li Y, Kuang K, Yang Z, Li J, Chen D, Li Y, Kou X, Zhong S. Oligomerization and photo-deoligomerization of HOOKLESS1 controls plant differential cell growth. Dev Cell. 2019:**51**(1):78–88. https://doi.org/10.1016/j.devcel.2019.08.007

Mazzella MA, Casal JJ, Muschietti JP, Fox AR. Hormonal networks involved in apical hook development in darkness and their response to light. Front Plant Sci. 2014:**5**:52. https://doi.org/10.3389/fpls.2014.00052

Millar AH, Heazlewood JL, Giglione C, Holdsworth MJ, Bachmair A, Schulze WX. The scope, functions, and dynamics of posttranslational protein modifications. Annu Rev Plant Biol. 2019:**70**(1):119–151. https://doi.org/10.1146/annurev-arplant-050718-100211

Miura K, Jin JB, Lee J, Yoo CY, Stirm V, Miura T, Ashworth EN, Bressan RA, Yun D-J, Hasegawa PM. SIZ1-mediated sumoylation of ICE1 controls CBF3/DREB1A expression and freezing tolerance in Arabidopsis. Plant Cell. 2007:**19**(4):1403–1414. https://doi.org/10.1105/tpc.106.048397

Morrell R, Sadanandom A. Dealing with stress: a review of plant SUMO proteases. Front Plant Sci. 2019:**10**:1122. https://doi.org/10.3389/fpls.2019.01122

Mukhopadhyay D, Dasso M. Modification in reverse: the SUMO proteases. Trends Biochem Sci. 2007:**32**(6):286–295. https://doi.org/10.1016/j.tibs.2007.05.002

Niu D, Lin XL, Kong X, Qu GP, Cai B, Lee J, and Jin JB. SIZ1-mediated SUMOylation of TPR1 suppresses plant immunity in Arabidopsis. Mol Plant. 2019:**12**(2):215–228. https://doi.org/10.1016/j.molp.2018.12.002

Osterlund MT, Hardtke CS, Wei N, Deng XW. Targeted destabilization of HY5 during light-regulated development of Arabidopsis. Nature. 2000:**405**(6785):462–466. https://doi.org/10.1038/35013076

Raz V, Ecker JR. Regulation of differential growth in the apical hook of Arabidopsis. Development. 1999:**126**(16):3661–3668. https://doi.org/10.1242/dev.126.16.3661

Ruzicka K, Ljung K, Vanneste S, Podhorska R, Beeckman T, Friml J, Benkova E. Ethylene regulates root growth through effects on auxin biosynthesis and transport-dependent auxin distribution. Plant Cell. 2007:**19**(7):2197–2212. https://doi.org/10.1105/tpc.107.052126

Rytz TC, Miller MJ, McLoughlin F, Augustine RC, Marshall RS, Juan YT, Charng YY, Scalf M, Smith LM, Vierstra RD. SUMOylome profiling reveals a diverse array of nuclear targets modified by the SUMO ligase SIZ1 during heat stress. Plant Cell. 2018:**30**(5):1077–1099. https://doi.org/10.1105/tpc.17.00993

Saitoh H, Hinchey J. Functional heterogeneity of small ubiquitin-related protein modifiers SUMO-1 versus SUMO-2/3. J Biol Chem. 2000:**275**(9):6252–6258. https://doi.org/10.1074/jbc.275.9.6252

Saleh A, Withers J, Mohan R, Marques J, Gu Y, Yan S, Zavaliev R, Nomoto M, Tada Y, Dong X. Posttranslational modifications of the master transcriptional regulator NPR1 enable dynamic but tight control of plant immune responses. Cell Host Microbe. 2015:**18**(2):169–182. https://doi.org/10.1016/j.chom.2015.07.005

Shi H, Lyu M, Luo Y, Liu S, Li Y, He H, Wei N, Deng XW, Zhong S. Genome-wide regulation of light-controlled seedling morphogenesis by three families of transcription factors. Proc Natl Acad Sci U S A. 2018:**115**(25):6482–6487. https://doi.org/10.1073/pnas.1803861115

Smet D, Žádníková P, Vandenbussche F, Benková E, Van Der Straeten D. Dynamic infrared imaging analysis of apical hook development in Arabidopsis: the case of brassinosteroids. New Phytol. 2014:**202**(4):1398–1411. https://doi.org/10.1111/nph.12751

Son GH, Park BS, Song JT, Seo HS. FLC-mediated flowering repression is positively regulated by sumoylation. J Exp Bot. 2014:**65**(1):339–351. https://doi.org/10.1093/jxb/ert383

Song S, Huang H, Gao H, Wang J, Wu D, Liu X, Yang S, Zhai Q, Li C, Qi T, et al. Interaction between MYC2 and ETHYLENE INSENSITIVE3 modulates antagonism between jasmonate and ethylene signaling in Arabidopsis. Plant Cell. 2014:**26**(1):263–279. https://doi.org/10.1105/tpc.113.120394

Srivastava M, Srivastava AK, Orosa-Puente B, Campanaro A, Zhang C, Sadanandom A. SUMO conjugation to BZR1 enables brassinosteroid signaling to integrate environmental cues to shape plant growth. Curr Biol. 2020:**30**(8):1410–1423.e3. https://doi.org/10.1016/j.cub.2020.01.089

Srivastava M, Srivastava AK, Roy D, Mansi M, Gough C, Bhagat PK, Zhang C, Sadanandom A. The conjugation of SUMO to the transcription factor MYC2 functions in blue light-mediated seedling development in Arabidopsis. Plant Cell. 2022:**34**(8):2892–2906. https://doi.org/10.1093/plcell/koac142

Stepanova AN, Yun J, Likhacheva AV, Alonso JM. Multilevel interactions between ethylene and auxin in Arabidopsis roots. Plant Cell. 2007:**19**(7):2169–2185. https://doi.org/10.1105/tpc.107.052068

Tada Y, Spoel SH, Pajerowska-Mukhtar K, Mou Z, Song J, Wang C, Zuo J, Dong X. Plant immunity requires conformational charges of NPR1 via S-nitrosylation and thioredoxins. Science. 2008:**321**(5891):952–956. https://doi.org/10.1126/science.1156970

Tian Y, Fan M, Qin Z, Lv H, Wang M, Zhang Z, Zhou W, Zhao N, Li X, Han C, et al. Hydrogen peroxide positively regulates brassinosteroid signaling through oxidation of the BRASSINAZOLE-RESISTANT1 transcription factor. Nat Commun. 2018:**9**(1):1063. https://doi.org/10.1038/s41467-018-03463-x

Wang Q, Lin C. Mechanisms of cryptochrome-mediated photoresponses in plants. Annu Rev Plant Biol. 2020:**71**(1):103–129. https://doi.org/10.1146/annurev-arplant-050718-100300

Wang Y, Guo H. On hormonal regulation of the dynamic apical hook development. New Phytol. 2019:**222**(3):1230–1234. https://doi.org/10.1111/nph.15626

Wu Q, Kuang K, Lyu M, Zhao Y, Li Y, Li J, Pan Y, Shi H, Zhong S. Allosteric deactivation of PIFs and EIN3 by microproteins in light control of plant development. Proc Natl Acad Sci U S A. 2020:**117**-(31):18858–18868. https://doi.org/10.1073/pnas.2002313117

Xiao Y, Chu L, Zhang Y, Bian Y, Xiao J, Xu D. HY5: a pivotal regulator of light-dependent development in higher plants. Front Plant Sci. 2021:**12**:800989. https://doi.org/10.3389/fpls.2021.800989

Xu X, Paik I, Zhu L, Huq E. Illuminating progress in phytochrome-mediated light signaling pathways. Trends Plant Sci. 2015:**20**(10):641–650. https://doi.org/10.1016/j.tplants.2015.06.010

Yang Y, Liang T, Zhang LB, Shao K, Gu XX, Shang RX, Shi N, Li X, Zhang P, Liu HT. UVR8 interacts with WRKY36 to regulate HY5 transcription and hypocotyl elongation in Arabidopsis. Nat Plants. 2018:**4**(2):98–107. https://doi.org/10.1038/s41477-017-0099-0

Yoo S-D, Cho Y-H, Sheen J. Arabidopsis mesophyll protoplasts: a versatile cell system for transient gene expression analysis. Nat Protoc. 2007:**2**(7):1565–1572. https://doi.org/10.1038/nprot.2007.199

Yu X, Li L, Li L, Guo M, Chory J, Yin Y. Modulation of brassinosteroid-regulated gene expression by jumonji domain-containing proteins ELF6 and REF6 in Arabidopsis. Proc Natl Acad Sci U S A. 2008:**105**(21):7618–7623. https://doi.org/10.1073/pnas.0802254105

Zhang D, Tan W, Yang F, Han Q, Deng X, Guo H, Liu B, Yin Y, Lin H. A BIN2-GLK1 signaling module integrates brassinosteroid and light signaling to repress chloroplast development in the dark. Dev Cell. 2021:**56**(3):310–324. https://doi.org/10.1016/j.devcel.2020.12.001

Zhang L, Han Q, Xiong J, Zheng T, Han J, Zhou H, Lin H, Yin Y, Zhang D. Sumoylation of BRI1-EMS-SUPPRESSOR 1 (BES1) by the SUMO E3 ligase SIZ1 negatively regulates brassinosteroids signaling in Arabidopsis thaliana. Plant Cell Physiol. 2019:**60**(10):2282–2292. https://doi.org/10.1093/pcp/pcz125

Zhang X, Henriques R, Lin S-S, Niu Q-W, Chua N-H. Agrobacterium-mediated transformation of Arabidopsis thaliana using the floral dip method. Nat Protoc. 2006:**1**(2):641–646. https://doi.org/10.1038/nprot.2006.97

Zhang X, Ji Y, Xue C, Ma H, Xi Y, Huang P, Wang H, An F, Li B, Wang Y, et al. Integrated regulation of apical hook development by transcriptional coupling of EIN3/EIL1 and PIFs in Arabidopsis. Plant Cell. 2018:**30**(9):1971–1988. https://doi.org/10.1105/tpc.18.00018

Zhang X, Zhu Z, An F, Hao D, Li P, Song J, Yi C, Guo H. Jasmonate-activated MYC2 represses ETHYLENE INSENSITIVE3 activity to antagonize ethylene-promoted apical hook formation in Arabidopsis. Plant Cell. 2014:**26**(3):1105–1117. https://doi.org/10.1105/tpc.113.122002

Zhang XY, Huai JL, Liu SR, Jin JB, Lin RC. SIZ1-mediated SUMO modification of SEUSS regulates photomorphogenesis in Arabidopsis. Plant Commun. 2020:**1**(5):100080. https://doi.org/10.1016/j.xplc.2020.100080

Zheng T, Li Y, Lei W, Qiao K, Liu B, Zhang D, Lin H. SUMO E3 ligase SIZ1 stabilizes MYB75 to regulate anthocyanin accumulation under high light conditions in Arabidopsis. Plant Sci. 2020:**292**:110355. https://doi.org/10.1016/j.plantsci.2019.110355

Zheng T, Tan W, Yang H, Zhang L, Li T, Liu B, Zhang D, Lin H. Regulation of anthocyanin accumulation via MYB75/HAT1/TPL-mediated transcriptional repression. PLoS Genet. 2019:**15**(3):e1007993. https://doi.org/10.1371/journal.pgen.1007993